Journal of Medicinal Chemistry

PERSPECTIVE

pubs.acs.org/jmc

How Well Can Fragments Explore Accessed Chemical Space? A Case Study from Heat Shock Protein 90

Miniperspective

Stephen D. Roughley[†] and Roderick E. Hubbard[*,†,‡]

[†]Vernalis (R&D) Ltd., Granta Park, Abington, Cambridge, CB21 6GB, U.K.

[‡]York Structural Biology Laboratory and Hull York Medical School, University of York, Heslington, York, YO10 5DD, U.K.

Supporting Information

1. INTRODUCTION

1.1. Fragments. The central idea in fragment-based discovery is that screening a target against a small number (as few as 500 compounds) of low molecular weight compounds (usually less than 250 Da) will identify a number of core motifs that can fit the target binding site. Although the fragment hits bind with low affinity (100s of μM), they are highly ligand efficient[1,2] and the past 5 years has seen an increasing number of compounds entering clinical trials that were derived from or inspired by fragments (for reviews see refs 3−5). The methods have also been extensively reviewed: the main elements of a fragment-based drug discovery platform are a fragment library,[6−8] a method (usually biophysical) for detecting and characterizing such weak binding[9−11] and a strategy for evolving the fragments into more potent hits and leads.[9,12] Three main approaches have emerged for integrating fragments with medicinal chemistry to optimize fragments to hits and leads: (1) Linking fragments together may be possible where there is more than one discrete binding site (such as the SAR-by-NMR approach from Abbott[13−16]). (2) Growing fragments has been successful either using the fragment to perform a substructure search of available compounds (so-called SAR-by-catalog) or by structure-guided addition of chemical groups.[17,18] (3) Finally, there has been some success with merging, where features of fragments and other hits are combined to design new hit compounds.[19−21]

1.2. Fragments, Size, and Chemical Space. At the core of the fragment-based approach is the tenet that a small number of fragments can sample an extremely large chemical space. A recent analysis[22] suggests that each additional heavy atom in a molecule increases over 8-fold the size of chemical space accessible by known synthetic chemistry. This means that screening a 1000 member library that averages 14 heavy atoms (MW 190) would be equivalent to screening a library of over 10^{18} molecules of 32 heavy atoms (MW 450). Clearly, there are many approximations and assumptions in that calculation, but it does emphasize that each fragment represents a massive number of larger compounds.

1.3. Introduction to Hsp90 as a Test Case. There has been considerable activity and success in a number of organizations in generating inhibitors and drug candidates against the molecular chaperone, heat shock protein 90 (Hsp90), as potential therapeutics to treat cancer, reviewed most recently in refs 23,24. These and other reviews describe the cellular and molecular biology of Hsp90 and the link to cancer. Here we provide a brief summary. The major cellular function of the Hsp90 family of chaperones is to aid the folding and thus maintain the integrity of a wide range of so-called "client" proteins in a cell. The most abundant isoform in the cytosol is dimeric Hsp90α which assembles into large multi-protein complexes with a variety of cochaperones.[25] Hsp90α is a member of the GHKL family of ATPases[26] and has three domains: an N-terminal domain (hereafter Nt-Hsp90) with an unusually shaped ATP binding cleft characterized by a left handed $\beta-\alpha-\beta$ (Bergerat) fold, a central domain that contributes to the catalytic activity but primarily consists of a hydrophobic cleft that is the site for recruitment of client proteins, and a C-terminal domain that is implicated in dimerization and has a role in autophosphorylation of the protein. The mechanism of the chaperone cycle is complex and not yet fully understood but requires the sequential binding of various cochaperones as well as the hydrolysis of ATP.[25]

Many of the proteins that are implicated in cancer, including mutated oncogenes, are Hsp90 clients, and early work with the natural products **1** (geldanamycin) and **42** (radicicol) and subsequently purine-derived compounds such as **4** (PU3)[27] established the potential for Hsp90 inhibitors[28] to affect all the hallmarks of cancer.[29] Although the middle domain of Hsp90 contributes to the catalytic cycle of ATP hydrolysis, the structure of the N-terminal domain alone has been sufficient to guide the early stages of designing inhibitors that target the ATP binding site. Figure 1 shows the structures of **1**[30] (Figure 1a) and **4**[31,32] (Figure 1b) bound to the ATP binding site in Nt-Hsp90. The purine cleft in the protein retains essentially the same conformation on binding of the different ligands, but the trimethoxybenzene moiety of **4** binds to an additional binding site that is formed by a change in the conformation of residues 110−115 (colored yellow) which we will refer to as the helical conformation. Figure 1c shows details of the interactions made by **4** in the binding site, most of which are common to all Hsp90 inhibitors. The key interactions are hydrogen bonds with the aspartic acid, D93, both directly and through a network of waters, and a stacking interaction with phenylalanine, F138. The position of leucine, L107 seen with **4** bound, is a signature for the helical conformation.

The first Hsp90 inhibitor to enter clinical trials was the semisynthetic ansamycin **2** (17-allylamino-17-demethoxygeldanamycin,[28] 17-AAG, tanespimycin). The compound has a number of issues including poor solubility, and although development of **2** has been

Received: March 25, 2011
Published: May 11, 2011

dx.doi.org/10.1021/jm200350g | J. Med. Chem. 2011, 54, 3989–4005

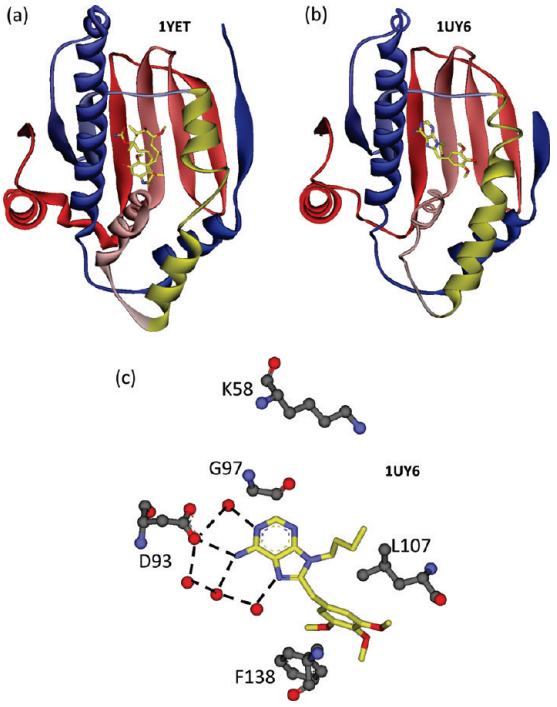

Figure 1. Crystal structures of Nt-Hsp90 showing secondary structure colored blue to red, N to C terminus with residues 100−124 in yellow in complex with (a) compound **1** and (b) compound **4**[80] shown in stick and (c) detail of compound **4** binding showing binding site residues (K58, D93, G97, L107, F138) and key water molecules. The four-letter codes in this and subsequent figures refer to the entries in the Protein Data Bank (http://www.rcsb.org).

halted recently, these early studies established a degree of validation, demonstrating that inhibition of the target showed evidence of target modulation in a range of cancers.[28,33] This has led to significant efforts by many organizations to identify novel, fully synthetic small molecule inhibitors of Hsp90, described later in this article.[23,34−39] Some of these drug discovery campaigns have exploited fragment based discovery, while others have used high throughput screening or design based on the known cofactor, ATP, with optimization often aided by structures of inhibitors bound to the target.

1.4. This Article. This extensive literature provides an opportunity to investigate how well the binding motifs and central scaffolds contained in the disclosed compounds are represented by the compounds identified in a fragment screening campaign.

2. VERNALIS FBDD PROJECT

The first Vernalis fragment screen against Hsp90 was carried out in 2002. A fragment screen requires three main components: a fragment library, a method able to detect low affinity binding, and a suitable sample of the target. The development of fragment libraries at Vernalis is well documented;[6,7] the first screen was performed with the initial 719 fragments (average MW 187) that made up the SeeDs1 library described in ref 6. The first published example of fragment screening that led to optimized candidate molecules was the SAR-by-NMR approach from Abbott.[13] This used protein-observed NMR methods, such as HSQC, to monitor the shift in peaks from labeled amides in the protein on titration with fragment(s). This approach has limitations on the size of protein system that can be studied (typically 30 kDa mass), so scientists at RiboTargets (a precursor company to Vernalis) had experimented with ligand-observed methods in earlier work to monitor ligand binding to ribosomal subunits (B. Davis, personal communication). These methods (such as STD[40]) monitor the change in the NMR spectrum from the ligands in solution arising from interactions with the protein. The first screen of 719 fragments monitored STD signals from ligands that were added in mixtures of 2 compounds at 1 mM each to a sample of Nt-Hsp90 at 10 μM. It is possible that signals arise from nonspecific binding at such high concentrations of fragments. Therefore, the spectra were measured again after addition of the known ATP-competitive ligand **4**[41] at 100 μM, and 17 hits were identified, defined as those fragments whose binding signal was suppressed by the competitor.

Following this early experience, improvements were made in both the fragment library[6] and the NMR protocols for fragment screening (as described in ref 42). A subsequent screen of the full 1350 fragments in the library (screened as mixtures of 12 compounds at 500 μM each) against Hsp90 identified a total of 60 fragments that were competitive with **4** and gave positive signals in all three NMR experiments (STD, Water-Logsy,[43] and CPMG[44]). The experience at Vernalis[7] on a range of targets is that this level of hit rate is consistent with being able to discover potent inhibitors of the target.

Five of the initial fragment hits were not seen in the second screen (one because it was no longer in the library; four because they did not give robust signals in all three experiments). Of the fragments discussed in this article, compounds **14**, **15**, **18**, **45**, **46**, **48**, **57**, and **66** were discovered from the initial fragment screen and only compounds **41**, **54**, **58**, **59**, **64**, and **67** came from the subsequent full screen. Although a crystal structure of compound **46** was obtained, it was not a hit in the full screen, suggesting that the binding is not robust at the approximately 5 mM affinity cutoff expected under the full screen conditions.

It is relatively straightforward to determine the crystal structure of ligands soaked into apo-Nt-Hsp90 crystals (with cocrystallization of some compounds to check for artifacts). All of the structural diagrams in this article are from crystal structures (see Supporting Information and the figures for the PDB file codes that contain data collection and refinement statistics for those structures newly revealed in this article and now deposited in the Protein DataBank, http://www.rcsb.org). The success rate of achieving crystal structures of fragments bound to Nt-Hsp90 was relatively high. Of the total of 65 fragment hits from the two screens, 33 structures were obtained at the first try at soaking for the 55 fragments for which attempts were made. There has been one instance (reported in ref 19 for compound **18**) where a different binding pose is seen in crystal structures from cocrystallization and from soaking, but this is rare.

3. PUBLISHED HSP90 INHIBITOR PROGRAMS

Janin[24] and Biamonte et al.[23] have recently published comprehensive reviews of the inhibitors and clinical candidates that have been disclosed as inhibitors of Hsp90. Janin categorized the compounds according to basic chemotype and binding mode; in this section we have grouped the compounds on their originator. This is summarized in Figure 2 for the compounds that have entered clinical trials and in Figure 3 for other compounds optimized from fragments for which preclinical data have been reported (note that **8** (CUDC-305, licensed to Debiopharm as Debio 0932)[45,46] and the structure of **13** (AT13387)[47] were disclosed since the Biamonte et al. review was assembled).

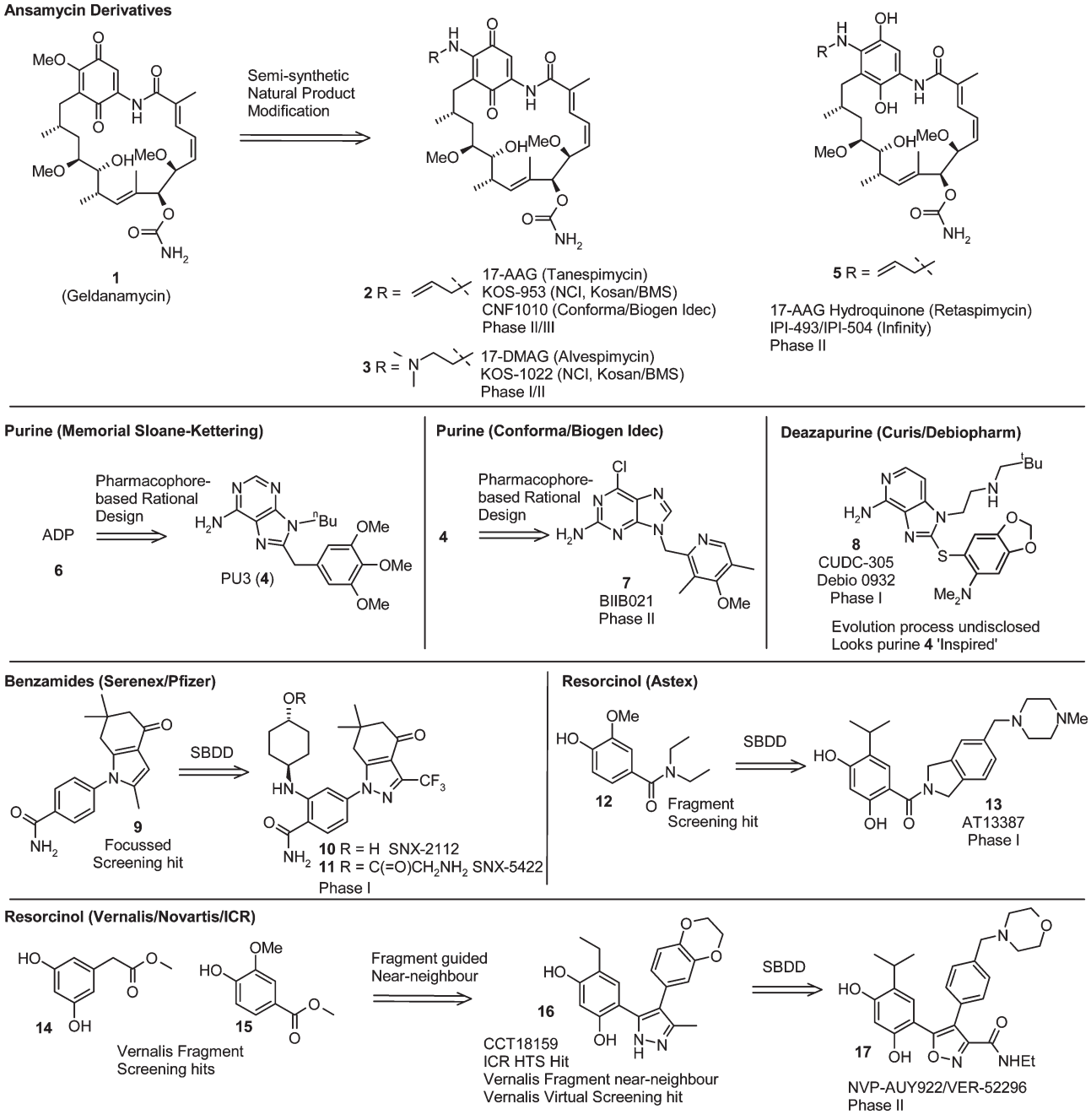

Figure 2. Summary of the origin and chemical evolution of known clinical candidate structures.

Supporting Information Table 1 provides information to link the different categorization for individual compounds. The following is a brief description for each class of compound.

3.1. Ansamycin Derivatives (Figure 2). Early work focused on semisynthetic derivatives of the ansamycin antibiotic **1**, centering on modification of the quinone 17-position methoxy group. Two compound structures resulted from these efforts; in both cases the methoxy derivative was replaced with an amine substituent, resulting in **2**, (KOS-953, CNF1010[48]) and the more soluble **3** (17-DMAG, alvespimycin, KOS-1022[33]). Later work resulted in the reduced form of the quinone moiety of **2** (retaspimycin, IPI-493/IPI-504, compound **5**[49]) also entering clinical trials. Progress with these compounds is reviewed in refs 23, 28, and 33.

3.2. Ligands Designed on a Purine Scaffold (Figure 2). The first reported fully synthetic Hsp90 inhibitor was **4**, first described by Chiosis et al.[27,41] They describe the design of the purine-based inhibitor based on examination of the X-ray crystal structures of **1** and ADP **6** and report similar cellular activities to **1** itself. A large number of variations on the structure of **4** have been published subsequently by a variety of groups (reviewed in refs 24 and 50). Workers at Conforma Therapeutics developed an alternative purine scaffold (which evolved into **7** (BIIB021)[51]), based on a pharmacophore derived from **4**, in which the purine motif is rotated (by moving the NH_2 substituent from the 1-position to the 3-position of the purine), and the hydrophobic pocket in the helical conformation is accessed from the N^7-position instead of the 8-position as seen in **4**.[51] In 2009,

dx.doi.org/10.1021/jm200350g |J. Med. Chem. 2011, 54, 3989–4005

Curis revealed the structure of **8** (which entered clinical trials in July 2010). Although no further detail was provided, the structure looks to be inspired by **4** and related compounds, with replacement of N^4 of the purine by carbon in an imidazo[4,5-*c*]pyridine ring system.[45,46]

3.3. Serenex Compounds (Figure 2). Serenex has described a benzamide bearing a tetrahydroindole substituent in the para-position (compound **9**), from a "purine-focused" HTS campaign. The compound was subsequently elaborated using a combination of molecular modeling and X-ray crystallography to generate the clinical candidate **10** (SNX-2112) and its glycine ester prodrug **11** (SNX-5422).[32,38] In these compounds, the pyrrole ring has undergone modification and an ortho-substituent introduced on the benzamide ring. Interestingly they identified that "the benzamide motif was likely to be a structural isostere for adenine".[52]

3.4. Resorcinol Containing Clinical Candidates (Figure 2). Workers at Vernalis, and more recently Astex, have independently reported fragment-based approaches to different resorcinol-based Hsp90 inhibitors, in both cases leading to compounds that have entered clinical trials for the treatment of a variety of cancers.[19,34,39] While both companies reported very similar phenolic fragment hits, different approaches were used to elaborate these to inhibitors with little in common except the key D93-binding resorcinol group. Interestingly, Pfizer (Figure 3) has reported resorcinol amide compounds very similar to **13**,[47] although there have been no reports of the Pfizer compounds entering clinical trials.

3.5. Vernalis Oral Candidate (Figure 2). Vernalis combined features from aminopyridine containing fragments (**18** and **19**) and virtual screening hits (**20** and **21**) in a structure-guided merging approach[19] to identify a designed thienopyrimidine fragment **22**. This fragment was then elaborated through structure-guided incorporation of chemical features from other virtual screening hits and the clinical candidate **17** (NVP-AUY922).[34,35] The resulting compound **23** (NVP-BEP800[19]) has subsequently entered preclinical assessment.

3.6. Astex, Evotec, and Abbott Aminopyridine Derived Inhibitors (Figure 3). Astex,[3,53] Evotec,[54,55] and Abbott[15] have all reported aminopyrimidine fragments similar to the Vernalis fragment **18** binding to D93 in the ATP site of Hsp90. Different approaches to fragment evolution have been described, resulting in very different inhibitors. Astex (fragments **38** and **39**) and Evotec (fragment **27**) both elaborated the fragments by a "growth" strategy, although neither company has reported compounds in these series entering preclinical development. Abbott (fragment **32**) actively sought a second-site binder (**33**), for which they observed two different binding modes depending on the technique used (X-ray crystallography and solution NMR). The structures were used to design links between the two fragments in the different binding modes, showing good overlay of the linked compounds with their fragment precursors. Evotec also described a third purine binding mode (fragment **29**), in which the purine N^7-H and N^4 form the donor−acceptor interaction proximal to D93 in the ATP binding site, in another fragment hit. In this case, the purine ring is acting more like a bioisosteric replacement of the aminopyrimidine motif seen in a number of other series (including the purines of both **4** and **7**). This fragment was linked to a second site binding fragment (**30**) by a flexible linker, giving a 1000-fold increase in potency.[55] As discussed later, both Astex and Vernalis obtained second site binding compounds from their fragment screens but did not elaborate the compounds further. These second site binders induce the helical conformation in Nt-Hsp90.

It is interesting to note that the variety of chemotypes seen binding to Hsp90 is not disimilar to that reported for the antibacterial target DNA gyrase, a related GHKL family member ATPase. Workers at Roche[56] identified a variety of aminopyrimidine-based fragments, phenols, and indazoles as hit compounds for the target, along with the carbamate-containing natural product inhibitor novobiocin.

4. SIMILARITY BETWEEN VERNALIS FRAGMENT HITS AND PUBLISHED INHIBITORS

The central question we are assessing in this article is to what extent the fragments identified in the Vernalis screen recapitulate the chemical substructures seen in the published Hsp90 inhibitors and the interactions made between the various compounds and the protein active site.

To perform this analysis, we have constructed Figures 4−9, which show details of the binding site residues and key water molecules in the crystal structures of sets of compounds bound to Nt-Hsp90. The Janin review[24] categorizes the compounds according to basic chemotype and binding mode. In this article, we define five main classes of compound by the central structural motif interacting with D93 as resorcinols (Figure 4), (benz)-amides (Figure 5), amino pyr(im)idine (Figure 6), phenol (Figure 8), and purine (Figure 9). In addition, we summarize the classes of compounds discovered through linking of two fragments (Figure 7) together. For each figure, we have selected representative fragments (primarily from Vernalis) and shown the structures alongside the structures of the clinical candidates or optimized fragment compounds. Each figure also includes an inventory of the PDB codes of deposited crystal structures for compounds of that class and a list of the compounds as numbered in the Janin review. Supporting Information Table 1 is a list of the chemical structures from the Janin review, with a note of which figure in that paper they appear, the PDB code (if a structure has been deposited), and which figure in this article contains the probable binding mode of that compound. Additional information on the generation of these lists is provided in Supporting Information.

The following section describes the structures observed. Section 5 will discuss how the chemical features provide ideas about isosteres and support for medicinal chemistry optimization.

4.1. Resorcinol Containing Compounds (Figure 4). The resorcinol (and as will be seen later, phenol) structural motif is found in many inhibitors discovered for Hsp90. Most resorcinols bind in the same position and orientation, bridging hydrogen bonds through solvent and to D93. The resorcinol substructure remains fairly constant as the fragments are evolved to full inhibitors, as can be seen in both the Vernalis (**17**)[35,39] and Astex (**13**)[39] clinical candidates and the strikingly similar preclinical compound from Pfizer (**26**).[47,57,58] Although the resorcinol motif was identified through medium throughput[59] and fragment and virtual screening,[60] the resorcinol motif was also apparent in the early crystal structures of the natural product **42** and is a constant feature of other natural products (such as **43** (pochonin D)) and "synthetic" natural products (pochoximes) such as **44**.[61]

Although the pose of the resorcinol motif remains constant with most substitution patterns, one exception has been

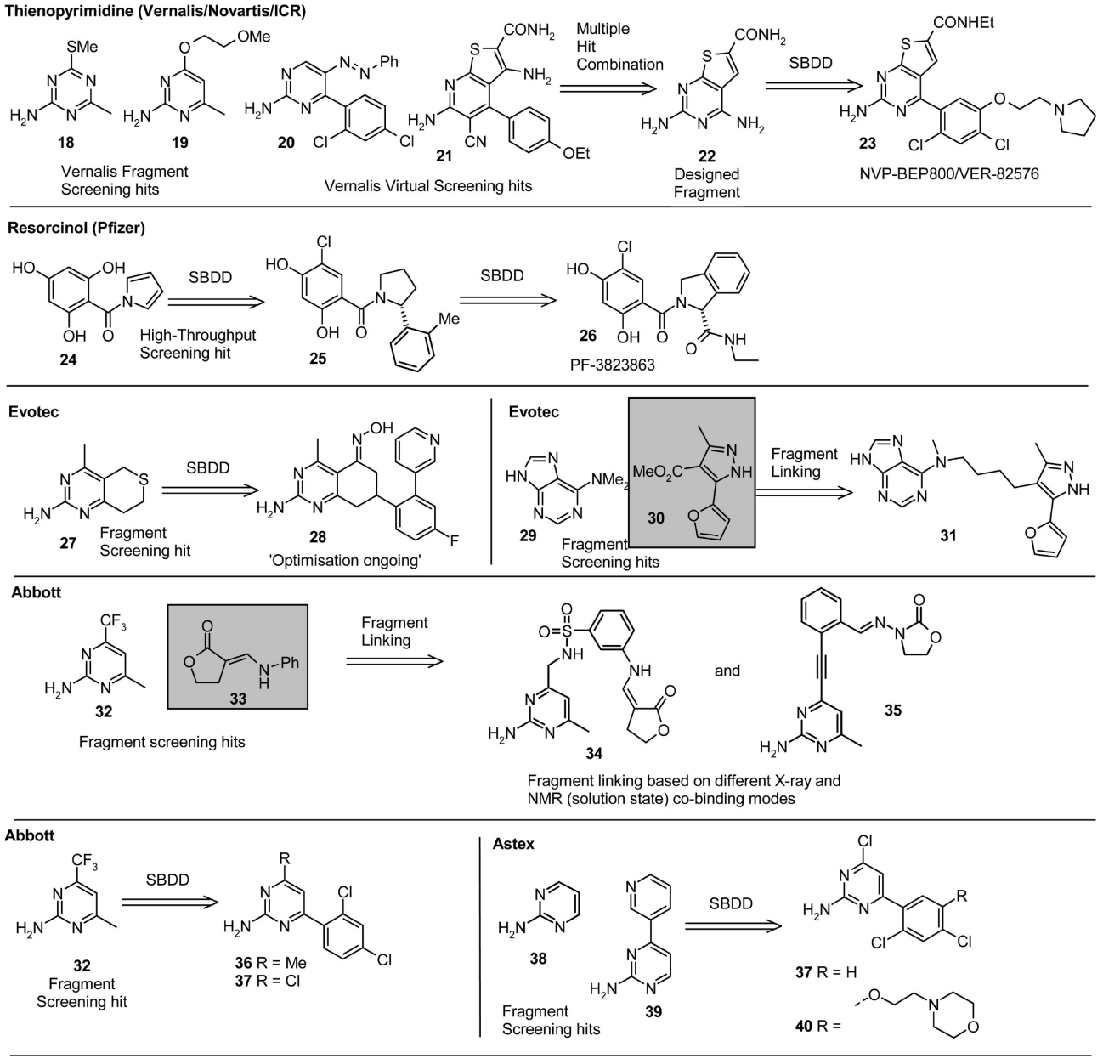

Figure 3. Summary of the origin and chemical evolution of known preclinical candidates, with second-site binding fragments on a shaded background.

observed in the crystal structure of compound **45**, where the methoxy substituent induces a shifted conformation with an additional water molecule interrupting the direct contact between D93 and the resorcinol. There is no clear structural rationale for this change in conformation, emphasizing that for some fragments, the energetic barrier to alternative poses is low, although discrete and unique conformations are seen in the electron density.

4.2. (Benz)amide Containing Compounds (Figure 5). The benzamide substructure in fragment **46** makes the same types of interaction with solvent and D93 as the other four structures of larger molecules shown in Figure 5. In both compound **3** and **50** (a bioengineered natural product[62]) the amide portion of a carbamate is making the same interactions with D93 and solvent as seen in the fragment. It is obviously a major leap of imagination to grow from the fragment **46** to compound **3**. However, compounds **47** and **49** (precursors of **10** currently in clinical trials with Serenex/Pfizer) both show an identical benzamide substructure linked through the amino group seen in fragment **46** and further substituted para to the benzamide to access the pocket region created in the helical conformation. Compound **48** was also identified as a hit in the first Vernalis fragment screen. It contains the same benzamide motif; however, it was one of the fragments for which a bound crystal structure was not obtained from initial soak or cocrystallization experiments.

4.3. 2-Aminopyr(im)idine Containing Compounds (Figure 6). Figure 6 shows the crystal structures of a number of compounds that include a 2-aminopyrimidine substructure. The important fragment is the aminopyrimidine **18** (and **19**) which binds in essentially the same position and orientation as the adenine containing a derivative of **4**, **52**,[31] the 2-aminopyrimidine containing compounds **7**,[51] **20**,[19] **23**,[19] and **53**,[63] and the 2-aminopyridine containing compound **21**.[19] Although **7** and **53** (a close analogue

dx.doi.org/10.1021/jm200350g |J. Med. Chem. 2011, 54, 3989–4005

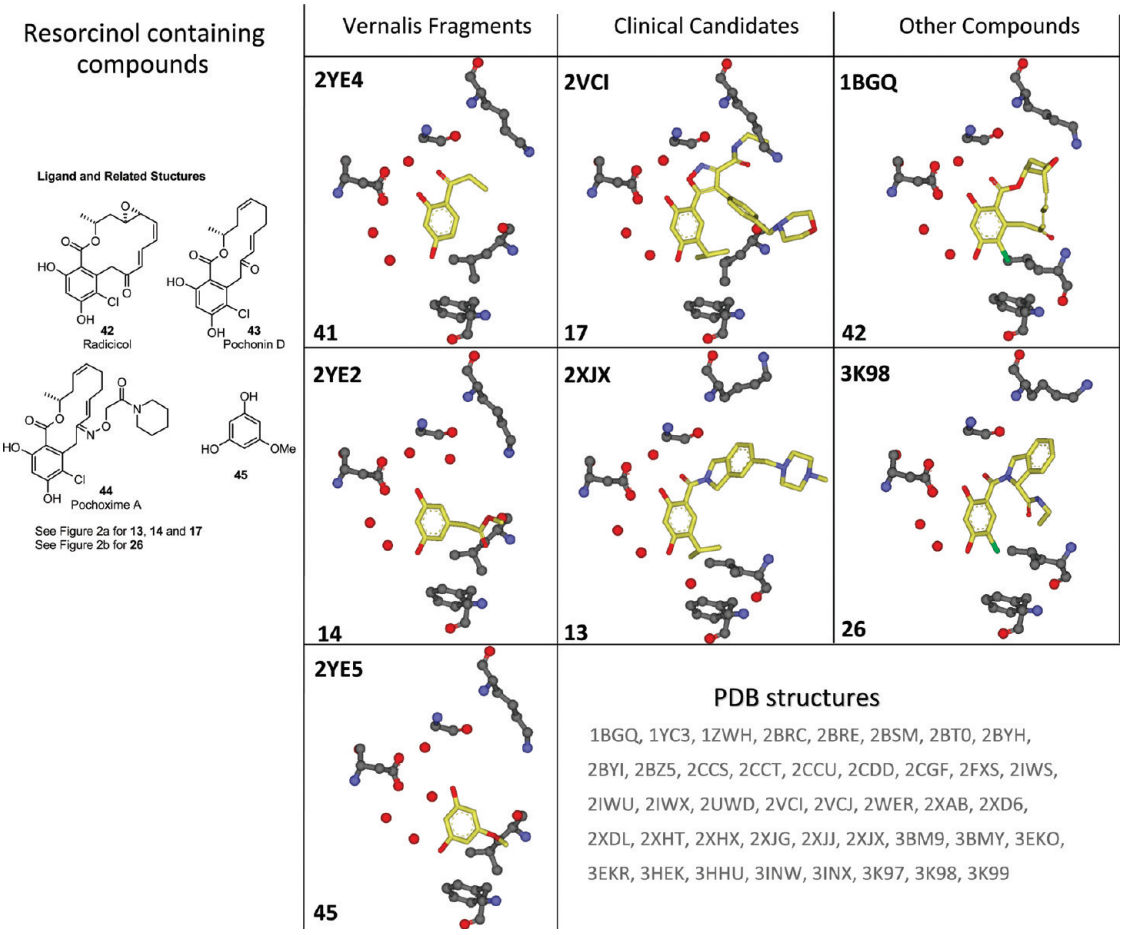

Figure 4. Resorcinol containing Hsp90 inhibitors. The panel of crystal structures of Nt-Hsp90 shows the binding site residues (see Figure 1) and key water molecules for representative fragments, clinical candidates, and other compounds. The four-character PDB codes are shown for each crystal structure. The area at the bottom lists the four-character PDB codes of all structures for this class of compound.

of **8**[45]) were discovered by non-structure-based optimization based on the chemical structure of ATP,[63] **23** was designed from the merging of structural information about both fragments and virtual screening hits (see above and ref 19). The 2-aminopyrimidine motif is also featured in compounds derived from linking fragments together (see Figure 7). Another interesting feature from this analysis is how the cyano group in **21** replaces the water molecule, one of the few examples across this data set where a substituent on the ligand displaces one of these highly conserved water molecules in the binding site. This is an example of the known replacement of an aromatic azomethine-type nitrogen atom hydrogen-bonding to water by a nitrile group, exploited in the design of a number of kinase inhibitors.[64,65]

4.4. Second Site Binding Compounds (Figure 7). The earliest successes of fragment-based discovery were from the Abbott group[13] who relied on protein-observed NMR methods for screening and structure determination. An initial screen identifies a fragment which is then optimized, with a second screen (usually of smaller fragments) conducted in the presence of that optimized fragment. After optimization of the second fragment, the structure of the complex is used to design linking strategies that connect the fragments. There have been some examples of success using this approach (as varied as stromelysin,[66] Bcl-2,[16] and the Hsp90 campaign described here[15]). However, many proteins do not present suitably distinct binding sites, and it requires considerable commitment in chemistry to synthesize compounds where the linking has not compromised the position and orientation of binding of the original fragment substructures.

The helical conformation of Nt-Hsp90 does have two binding sites available, and the Vernalis fragment screen identified compound **54** that binds in the hydrophobic cleft under the helix in the position occupied by trimethoxybenzene in **4**. This binding site does not exist in the apo-structure but can be induced in the crystal by soaking fragment **54** into apo-crystals. A number of structures were obtained at Vernalis with different fragments (e.g., **14** and **18**) bound at the same time as **54**. The electron density supports two alternative binding modes for fragment **54** when binding on its own; the orientation shown in Figure 7 is the minor conformation (~30% occupancy) which is similar to that reported as the unique binding orientation by Evotec for a similar compound (**30**). However, the orientation of **54** changes to the major conformation when other fragments are present (as also reported by Evotec). Plans were devised to link **14** and **54**, but other optimization strategies were judged to be more effective, so compounds were not made.

Interestingly, a number of others have reported the same second site binding phenomenon. Astex identified **38** and **55** as binding together but have not disclosed any optimized compounds.[53] Both Evotec (compound **31** from fragments **29** and **30**[55]) and Abbott (compound **35** from fragments **32** and **33**[15])

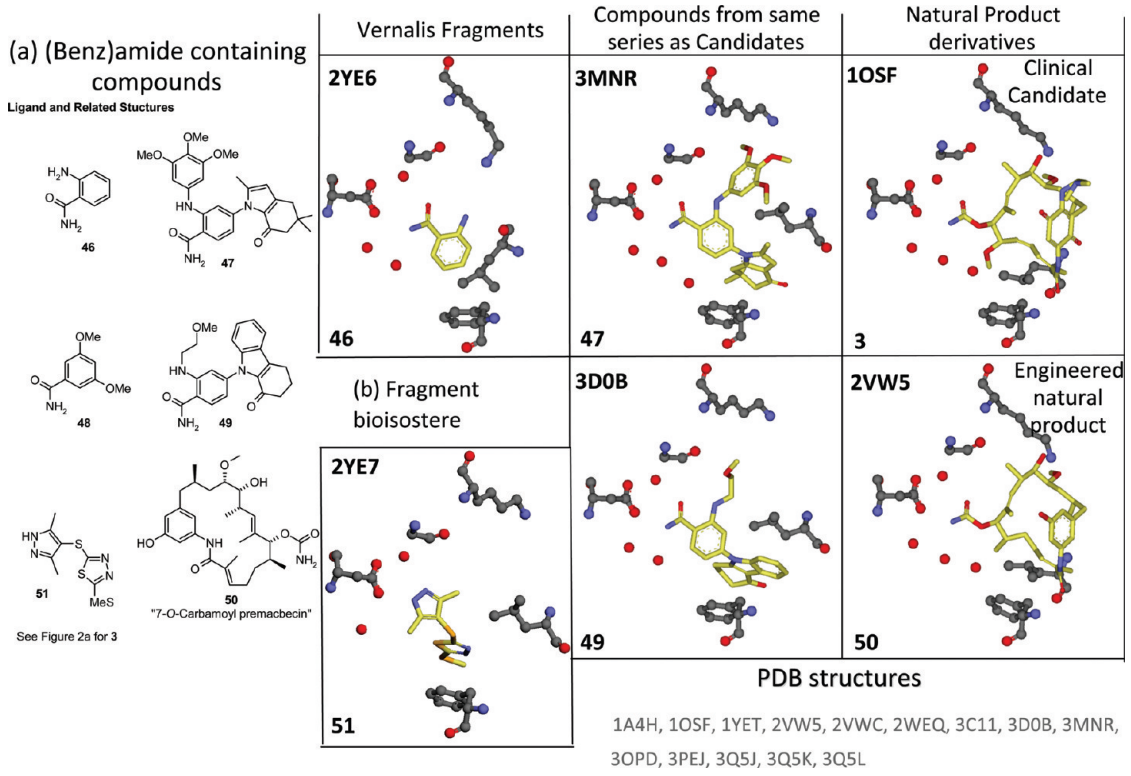

Figure 5. (a) (Benz)amide containing compounds and (b) a fragment that contains an amide bioisostere. The panel of crystal structures of Nt-Hsp90 shows the binding site residues (see Figure 1) and key water molecules for representative fragments, clinical candidates, and other compounds. The four-character PDB codes are shown for each crystal structure. The area near the bottom lists the four-character PDB codes of all structures for this class of compound.

synthesized optimized compounds that successfully linked the fragments from the two sites together. The linkers maintained the orientation and position of the original fragments. However, these compounds would require further optimization to achieve the affinity required to be considered as candidates and no further optimization has been reported to date.

4.5. Binding Mode of Phenol Containing Compounds (Figure 8). Compound **14** is an archetypal resorcinol, with one phenolic OH interacting directly with D93, the other phenolic OH indirectly via a water molecule. The consequences of disrupting one or other of these phenolic OH groups in some phenol containing fragments are shown in Figure 8. The phenolic OH remaining in the 2-methoxyphenol fragment **15** makes the same solvent bridged interaction with the same pose and interactions maintained for the similar Astex fragment **12**.[53] There is no direct interaction with D93, but there is an additional solvent bridged interaction through the carbonyl oxygen at the 4 position (an ester in the Vernalis fragment **15** and an amide in Astex fragment **12**). When this carbonyl oxygen is replaced by a hydroxymethyl at the 4-position (as in fragment **57**), the fragment flips its orientation. Now the phenolic OH is making a direct interaction with D93, and the methoxy and hydroxymethyl are making a solvent-bridged interaction. This same direct interaction with D93 is seen from the β-naphthol OH group in the virtual screening hit **56**.[60] Interestingly, there are no other substituents on this β-naphthol ring to interact with solvent, but further interactions are made by the other phenolic OH. Although the phenolic OH of **56** is shifted by some 1.3 Å relative to the ester carbonyl oxygen in **12** and **15**, these different atoms are able to make an equivalent solvent bridged interaction with D93.

The structures of a number of fragments bound to a protein can suggest ways of merging chemical features into improved fragments or compounds. There have been a number of examples where successful merging of such features has generated potent inhibitors.[19−21] The poses of the fragments seen in the crystal structures in Figure 8 suggest that combination of compounds **14** and **15** captures the key features of the natural products **42** and **43**, as emphasized in schematic I of Figure 8. In addition, the analysis also shows that such a hybrid accounts for many of the resorcinol-based series that have been published to date, such as the key features of the resorcinol amide and heteroarylresorcinol inhibitors (compounds **17**, **26**, and **42**; Figure 4) shown in Figure 4. In retrospect, it is now possible to see how the extended set of phenol-based fragments (**14**, **15**, **41**, and **45**) provide a consensus map (**62**) of the "allowed" vectors from the resorcinol binding motif which could be used to guide selection of compounds from substructure-based "SAR-by-catalog" approaches, as illustrated in schematic II of Figure 8.

The flip in orientation of the phenolic OH/methoxy substructure between fragments **15** and **57** is perhaps due to the enhanced strength of the solvent bridged interaction to be made by the ester carbonyl group in **15**. However, the changes do emphasize how quite subtle changes in the chemistry of a fragment can induce a change in compound orientation. A further example can be seen in the series of compounds **58**, **59**, and **60**. The phenolic OH of the Vernalis fragment **59** makes a direct interaction with D93, with the NH of the fused pyrazole ring making the solvent bridged interaction. These interactions are preserved in the evolved compound **60** published by Astex,[39] this time through a fused dihydropyrrole ring. However, the

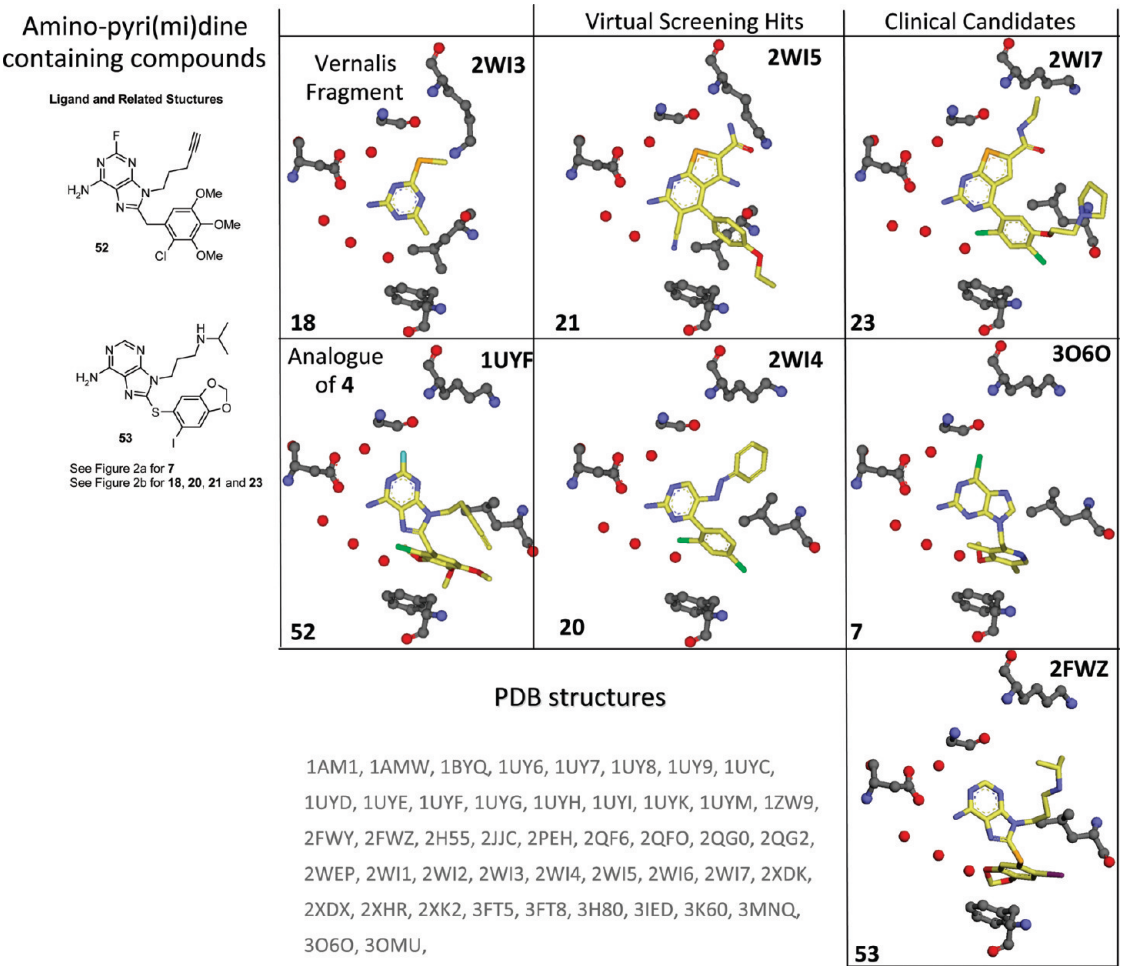

Figure 6. Aminopyri(mi)dine containing compounds. The panel of crystal structures of Nt-Hsp90 shows the binding site residues (see Figure 1) and key water molecules for representative fragments, clinical candidates, and other compounds. The four-character PDB codes are shown for each crystal structure. The area at the bottom lists the four-character PDB codes of all structures for this class of compound.

Vernalis fragment **58** differs only in the lack of a methyl substituent, and yet the binding orientation is completely flipped. A single heavy atom change (3-Me ↔ 3-H) results in a dramatic change in the binding mode of the fragment. This is characteristic of weakly binding fragments and demonstrates again the care that is required in following up iterations of fragment evolution and elaboration with structural data (see ref 19).

4.6. Binding Mode of Pyrimidine Containing Compounds (Figure 9). Some of the early ligand-based design strategies for identifying inhibitors of Hsp90 (such as the purine-derived series from Chiosis (such as compound **53**[63] and the Serenex/Pfizer series, compounds **10** and **11**[32,38]) were based on the adenine moiety of **6** (ADP). Figure 9 shows some representative fragments containing pyrimidine substructures. The position and orientation of binding of 4-aminopyrimidine are preserved across the fragments **64** and **63** and the structure seen for ADPNP (**65**) and the compounds derived from **4** such as **53** (see Figure 6). The amino moiety also makes the same interactions in the 2-aminopyrimidine fragment **18**. However, removal of the amino functional group (as seen in fragments **66** and **67**) results in a flip of the fused heterocycle, also seen by Evotec for both their fragment (**29**) and linked hit (**31**) compounds. These changes can be rationalized quite simply. For the example of **64** and **66**, both compounds only have one D−A pair. In the case of **66** the fragment is using N^4 and N^7-H, and for **64**, it is using the 1-NH_2 substituent and N^2. However, **66** lacks a 1-NH substituent and **64** has an N^7-Et group, so in both cases, the alternative binding mode is not available. In fragment **63**, both binding modes are available, but the electron density from the refined crystal structure clearly shows an ADPNP mode of binding. In contrast, purine **67**, which still possesses both a 1-NH substituent and an N^7-H, binds in the same orientation as **66**, the *N*-alkyl substituent presumably preventing the alternative binding mode from being accessed on steric grounds.

4.7. Conclusions. In summary, the key D93-binding cores of all the current compounds in clinical trials with known structures are well represented by the fragment screens performed at Vernalis. Strikingly, just 5 fragments from the 17 identified from the first screen of 719 compounds represent the core motifs of all the clinical candidates shown in Figure 2. This suggests that for Hsp90 at least, the fragments do cover an appropriate chemical space; what is then important is the imagination of the chemist in evolving the fragments into potent inhibitors.

The analysis presented above also highlights some important observations about fragment binding. Although the binding mode for a fragment can be preserved as the fragment is evolved or grown, just small modifications to the fragment can result in quite different binding modes. This emphasizes the desirability to

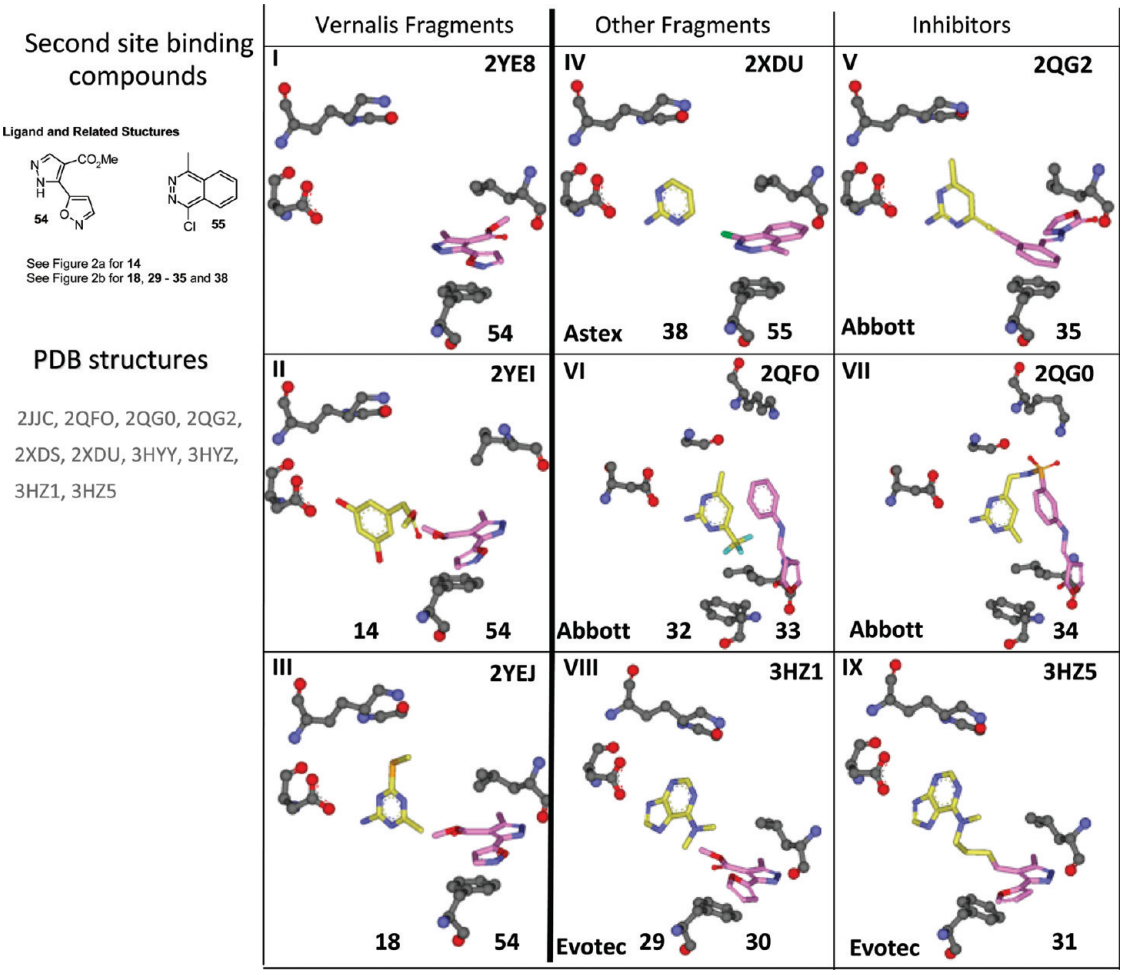

Figure 7. Second site binding compounds. Water molecules are excluded for clarity. The panel of crystal structures of Nt-Hsp90 shows the binding site residues (see Figure 1). The four-character PDB codes are shown for each crystal structure. The area at the bottom lists the four-character PDB codes of all structures for this class of compound. Panels I—V are in the same view. The views in the pairs of panels VI and VII and panels VIII and IX are adjusted for clarity.

determine as many structures as possible during the early stages of assessing and evolving fragments to ensure that a robust model is developed from which to optimize the compounds. Most fragment-based discovery campaigns have relied on X-ray crystallography to deliver the required throughput of protein—ligand complex structures. Although NMR methods can generate structural information (either full structures or information on key interactions from which reliable models can be built of compound binding pose), they take considerable resource and there are strict requirements on the protein system (assignment of spectrum, size of protein, etc).

The structures presented in Figures 4—9 also prompt three other interesting areas for discussion: how fragments can suggest bioisostere replacements, some thoughts for fragment library design, and some comments on how similar fragments can be optimized into very different lead compounds in different organisations.

5. BIOISOSTERES

The examples discussed so far in this Miniperspective have demonstrated how a fragment screen has identified the central core motif that either led to or is found in published optimized compounds. In this section we discuss how fragment screening provides insights into the broader range of chemotypes that can bind to the target of interest and provide ideas for bioisosteres. Two classes of bioisostere are considered. "Classical" bioisosteres are those that are part of the existing medicinal chemist's lexicon of obvious chemical replacements. "Cryptic" bioisosteres are less obvious and are derived from combinations of chemical features from different fragments and could provide ideas for moving into significantly different areas of chemical (and IP) space to that occupied by current known inhibitors.

5.1. Classical Bioisosteres (Figure 10, Panels I and II). Fragments **14** and **41** show the key features of the resorcinol binding mode exploited in a number of reported series of Hsp90 inhibitors: principally, two phenolic groups forming multiple hydrogen bonds with the protein, both directly and via the network of conserved water molecules within the binding site, and the hydrogen-bond acceptor carbonyl oxygen group (see Figures 4 and 8). Comparison of the bound structure of **14** with the hydroxyindazole **59** shows the 7-OH group of **59** to overlay with the *o*-OH group of **14**. This is an example of the classical phenolindazole bioisosteric replacement, in which the H-bond donor and acceptor functionalities of the phenolic OH group are separated onto NH1 and N2, respectively, in the indazole, as seen for gyrase,[56] Lck,[67] and PI3[68] kinase. In this case, the 1*H*-indazole

dx.doi.org/10.1021/jm200350g |*J. Med. Chem.* 2011, 54, 3989–4005

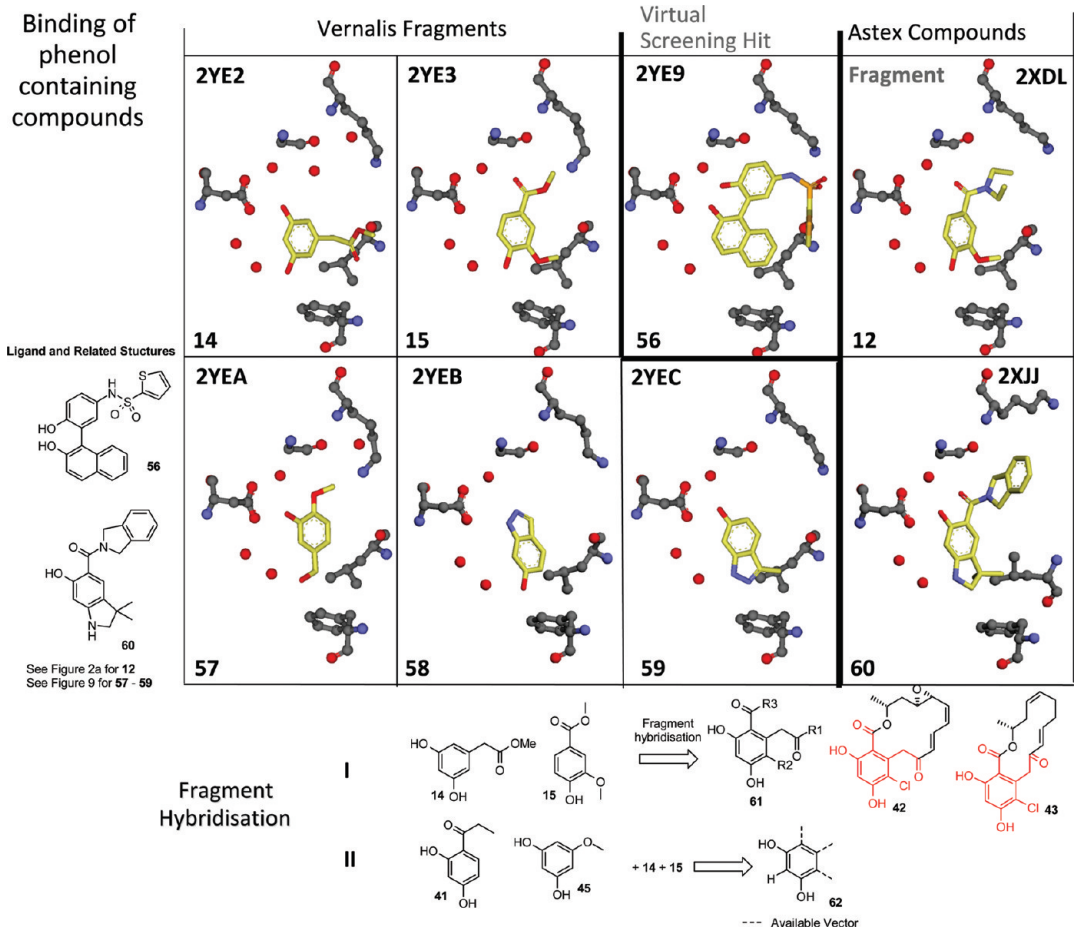

Figure 8. Binding of phenol containing compounds. The panel of crystal structures of Nt-Hsp90 shows the binding site residues (see Figure 1) and key water molecules for representative fragments, clinical candidates, and other compounds. Schematics I and II illustrate how hybrids of fragments account for various phenol and resorcinol containing compounds, as discussed in the text.

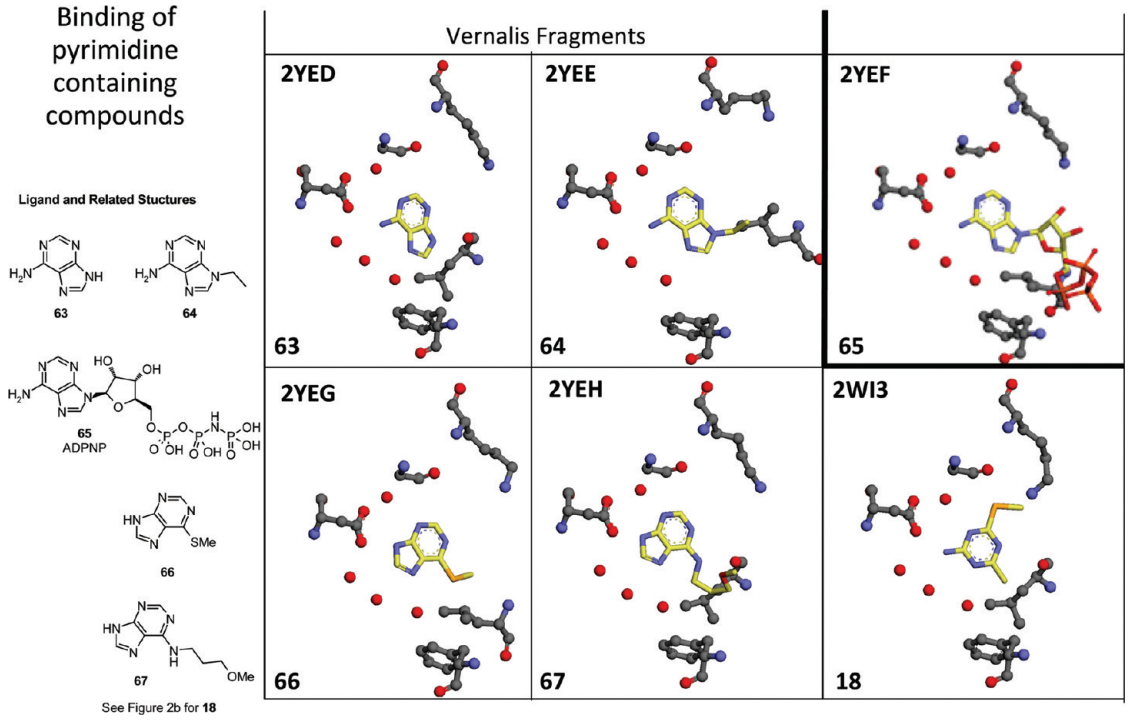

Figure 9. Binding of purine containing compounds.

dx.doi.org/10.1021/jm200350g |J. Med. Chem. 2011, 54, 3989–4005

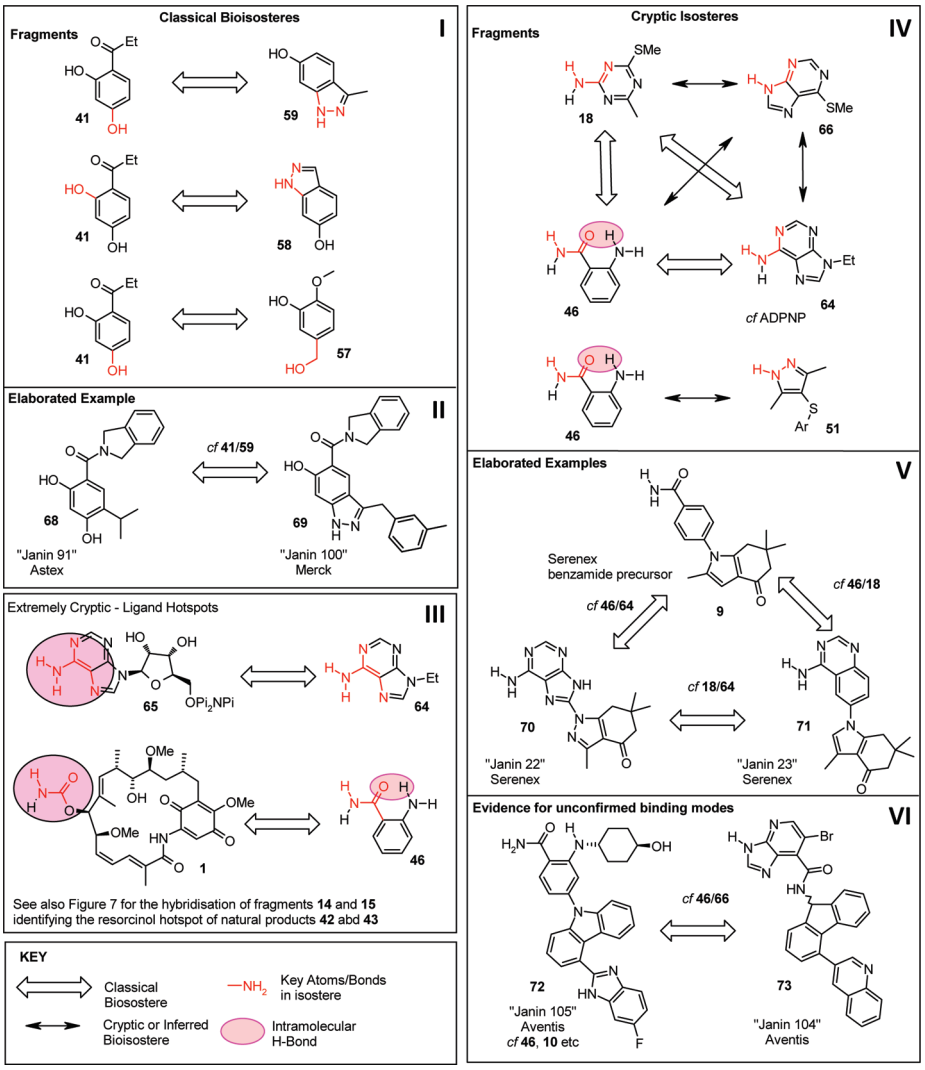

Figure 10. Bioisosteres: examples of simple classical bioisosteres identified by fragments (I) and selected elaborated examples (II), along with cryptic bioisosteres and their applications (IV−VI) and ligand hotspots (III).

NH provides the required H-bond donor functionality of the *p*-OH group of **14**, while the H-bond acceptor is not required to complete the hydrogen-bonded water network.

Comparison of **14** with the indazole fragment **58** (which lacks only the 3-methyl group of **59**) shows a second example of the phenolindazole bioisostere. In this case, however, the binding mode of the indazole has "flipped" such that it is the *o*-OH of **14** that is replaced by the indazole isostere, while the *p*-OH is overlaid closely by the 7-OH of **58**. The NH1 provides the H-bond donor interaction with D93, matching that of the *o*-OH of **14**, but additionally, N2 provides an H-bond acceptor located close to that of the carbonyl C=O of **14** (see also **15**). An example of this isosteric replacement in elaborated compounds is given by comparison of **68** (from Astex[39]) and the related Merck compounds such as **69** (patents in refs 212−214 in the Janin review[24]), in which the indazole amide replaces the resorcinol amide group.

A further example of a classical biostere within the resorcinol series of compounds is demonstrated by fragment **57**. Here, the *p*-OH of **14** is replaced by an extended $-CH_2OH$ substituent. This is a classical replacement, widely used in the area of catecholamine drug discovery. It serves to prevent rapid in vivo deactivation of the catechol-containing molecules and is expected to have considerable effects on the physicochemical properties of the molecule.[69,70] The relatively acidic phenol (typical pK_a of 8−11) is replaced by an aliphatic alcohol which is much less readily ionized (typical pK_a of 15−16). Closer comparison of the bound structures of **41** and **57** emphasizes an important feature of the fragment-based approach. In **57**, the aromatic ring has pivoted around the *o*-OH to a small extent in order to position the CH_2OH almost exactly overlaying the *p*-OH position in the binding site, thus maintaining the optimal H-bonding network. This pivoting of the binding motif would be difficult to achieve in a more heavily decorated molecule (for example, that incorporate the C=O from **41**) because of steric clashes with the binding site. The fragments therefore allow these alternative orientations to be explored before elaboration locks down the binding mode.

5.2. Cryptic Isosteres (Figure 10, Panels IV−VI). The structure of the aminotriazine fragment **18** (Figure 9) bound to Hsp90 provides an example of how comparison of the structure with other fragments generates ideas for nonobvious isosteric replacements. The key interactions are again the D−A pair

dx.doi.org/10.1021/jm200350g |*J. Med. Chem.* 2011, 54, 3989–4005

interaction with D93 both directly and via a conserved water molecule. The simplest example in this group is the comparison with the *o*-aminobenzamide structure **46** (Figure 5); in this case the D−A pair is provided by a primary amide. This replacement is a variation on the classical bioisosteric theme of ring replacement, in which a ring (normally part of a pair of fused rings) is replaced by an acyclic variant, in which the ring is effectively mimicked by an intramolecular H-bond as seen in **46**[71,72] The monocyclic nature of **18** is the principal reason for the nonobvious nature of this particular pairing (if **18** were part of a fused structure, e.g., a 4-aminoquinazoline, there would be little surprise in this replacement). Similarly, **46** is related to the purine **64** by an intramolecular H-bond/ring replacement, although in this case, the benzene ring of **46** has also been replaced by the imidazole ring of the purine, resulting in a "multistep" cryptic bioisostere.

Comparison of the bound structures of **18** and the purine fragments **64** and **66** (Figure 9) provides another set of examples. The aminotriazine of **18** closely overlays the pyrimidine ring of the purine **66** with the D−A pair provided by N^4 and N^7(H) of the purine nucleus. In the case of the second purine fragment, **64**, the ring fusion is 2,3- to the NH_2 group of **18**, recapitulating the purine binding mode seen in ADPNP and purine-derived compounds (e.g., **52** in Figure 6) . As with the replacement of **18** with **66**, this fusion requires an additional heteroatom translocation. Fragment **51** shows an alternative cryptic isosteric replacement for the D−A pair in this set, in this case through adjacent N atoms of a pyrazole ring. Classical heterocyclic isosteric replacements of esters and amides tend to have placed the heteroatoms in a 1,3-relationship, similar to that seen in the amide itself.[72,73]

The structures therefore explain the bioisosterism shown by **18** to **46**, **64**, and **66**, despite the less direct or obvious nature of the replacement. Indeed, this relationship (**46** ↔ **64**) was referred to by Serenex in papers describing early compounds leading to **47**.[32,38] However, this group of compounds (**46**, **64**, and **66**, along with **51**) are all bioisosteric with each other. We refer to this as "cryptic bioisosterism", as the pathway between any two of these structures is nontrivial and we consider extremely unlikely to be suggested during a conventional drug discovery program. It is also interesting that while the positions of D93, G97, and F138 remain unchanged throughout this series of structures, K58 and L107 show significant movements in order to accommodate the bound fragments, a conformation required for second-site binders (see section 4.4). Comparisons of the compound **47** (a precursor to the Serenex compound, **10**) with compounds **70** and **71** (Janin compounds **22** and **23**, respectively; Figure 10, panel V) show replacement of the benzamide group with aminopurine and aminoquinazoline motifs, in transformations analogous to the transitions from **46** to **64** and **18**.

Janin tentatively (Janin described the assignment as "risky") assigned the binding modes of a number of Aventis compounds (Janin compounds **102**−**105**; examples are compounds **72** and **73**) based on the *o*-aminobenzamide motif held in common with the Serenex inhibitors, presumably assuming that the 4-arylcarbazole would overlay with the 4-arylfluorenyl group in **73**. Further support is given to this hypothesis by comparison of fragments **46** and **66**, as shown in Figure 10 (panel VI). This demonstrates a further powerful feature of fragment-based methods; seemingly disparate structures of unknown or uncertain binding mode can be grouped together by comparison with known fragment overlays, allowing the assignment of otherwise obscure binding modes with some certainty.

5.3. Cryptic Isosteres: Ligand Hotspots (Figure 10, Panel III). A number of publications highlight the use of fragment screening approaches to identify ligand-binding hotspots on a target.[74−76] For Hsp90, the Vernalis fragment screens and those reported by others[15,53,54] all indicate a primary fragment-binding hotspot within the ATP-site centered around D93. Fragments have also identified additional, sometimes "cryptic" second pockets (again including second-site binders in Hsp90, which bind in the pocket formed in the helical conformation). However, taking the cryptic bioisosterism concept to an extreme, one can also consider a ligand-centric view, as opposed to the target-centric view. Thus, when presented with a crystal structure of a target in complex with endogenous or exogenous natural product ligands (e.g., ATP, **1**, **42**, and **43** in Hsp90), it can be difficult to identify which of the many interactions are crucial to ligand binding, particularly for targets where the structural biology is less well understood and there are only small numbers of characterized ligands. Comparison of the structures of fragments **18** and **64** with the bound structure of **65** (ADPNP) identifies the $N^2-C^1-C^6-N^9$ edge of the adenosine ring as the hotspot of this complex ligand (just 5 of the 31 heavy atoms of **65**). Similarly, comparison of the bound structures shows an exact overlap of the primary benzamide of **46** with the $-C(=O)NH_2$ atoms of the carbamate of **1**, highlighting the carbamate D−A pair as key to the binding of **1** to Hsp90. The carbamate thus represents the binding hotspot of the complex ligand, just 3 of the 40 heavy atoms in **1**. Earlier discussion in a number of sections above has highlighted the importance of combining information from multiple fragments. This ligand-centric approach gives results consistent with those seen when considering the whole ensemble of Hsp90-binding fragments, that D93 and its associated water-mediated H-bond network are key to ligand binding.

5.4. Bioisosteres: Summary/Conclusions. From the above, it is clear that fragments can serve as the inspiration for the development of bioisosteric replacements, which could potentially be applied to existing lead series discovered by fragment-based or other methods. In addition to suggesting "obvious" classical bioisosteres, the fragments are information-rich, in some cases suggesting modifications to the connecting groups to maintain optimal interactions between the ligand and protein. Additionally, we have shown the power of fragments to suggest more complex "cryptic" isosteric replacements. These are unlikely to be suggested without the additional insight and confidence provided by the crystal structures of ligands binding to the target.

6. FRAGMENT LIBRARY DESIGN

There has been considerable interest over the past few years in the design of libraries for fragment screening.[6−8,77] Although it is clear that keeping the molecular weight of compounds low (see section 1.2) increases the relative size of chemical space covered, there is some debate about the optimum number of compounds that should be screened. Most practitioners have found that careful quality control is required to maintain the library for effective screening at the high concentrations required. In addition the number of hits found (typical hit rates between 3% and 5% of the library) can place considerable demands on hit validation. For these reasons, most reported fragment libraries contain only 500−5000 compounds.

The analyses reported here emphasize the dilemma in limiting the number of fragments in a library. Although a carefully chosen, small library may sample most of the possible chemotypes that

can bind to a target, closely related fragments can adopt quite different "stable" binding modes, which can be viably elaborated to potent inhibitors. For example, the purine **63** is the simplest of the purine structures in Figure 9 and is capable of adopting either of the binding modes seen in fragments in this figure. However, its selection as a sole representative of "purines" would result in missing the second binding mode. As in any screening paradigm, there will be many missed compounds, but this does emphasize two points. The first is to maintain and screen as large and diverse a fragment library that can be maintained by the resources available. The second is to expand the SAR around the initial fragment hits with very close relatives and determine as many crystal structures as possible, before developing and committing to detailed chemistry optimization plans.

7. SIMILAR FRAGMENTS CAN GIVE DIFFERENT LEAD COMPOUNDS

A concern raised by some about fragment-based drug discovery approaches is that most fragment libraries are derived from a relatively small number of commercially available compounds. It is therefore likely that different organizations will obtain similar fragment hits for a target. Figures 4−9 compare the structures of some of the fragments disclosed from four different campaigns (at Astex,[53] Vernalis,[6,19] Evotec,[54] and Abbott[15]) against Hsp90. It is interesting to compare the nature of the fragment hits and the resulting lead compounds.

7.1. Phenols/Resorcinols. Interestingly, only Vernalis and Astex disclose phenols and resorcinols as fragment hits, although this substructure is the key binding motif in many hits against this target from natural products (**42**), virtual screening,[60] and high throughput screening.[59] Some medicinal chemists would exclude resorcinols from a screening collection because of their unfavorable DMPK properties, as the compound class is usually rapidly cleared by glucoronidation.[47,78,79] However, this property may be an advantage for Hsp90 inhibitors, giving rapid clearance from "normal" tissue. Vernalis and Astex report different, though similar compounds, and the binding modes (as shown in Figure 8) are essentially identical. Although the two companies converged on the same core of an isopropylresorcinol in the final clinical candidate, the rest of the compound is quite different.

7.2. Aminopyrimidines. All four companies have disclosed fragments containing or suggestive of this motif. As shown in Figures 6 and 9, Vernalis discovered a number of pyrimidine, aminopyrimidine, and pyridine containing fragments and compound series[19,80] that provided the starting point for design of the thienopyrimidine clinical candidate **23**. This remains the only example of this particular evolution route.

In stark contrast, three of the companies optimized (as shown in Figure 3) to an identical tricholorobiaryl template, compound **37**. The Astex fragment screen[39,53] identified an unsubstituted aminopyrimidine (compound **38**, Figures 2, 3, and 7) and published some SAR that developed a different vector to that explored in **23**. Abbott similarly optimized an aminopyrimidine fragment **32** to the potent hit **37**, and Vernalis arrived at exactly the same compound in one as yet unpublished series.

There are also examples of similar fragments leading to very different evolved compounds that still retain the core scaffold. Evotec identified an aminopyrimidine fused to various saturated ring systems from a fragment screen followed by SAR-by-catalog to generate a lead series for further optimization.[54] Evotec also identified a substituted purine (**29**) in the ATP binding site that adopts the same binding mode as seen by the Vernalis fragment **67**. Evotec also determined the structure of this purine with a pyrazolefuran moiety (**30**) bound in the hydrophobic pocket of the helical conformation. Subsequent linking gave compound **31**.[55] A rather similar second site binding fragment was discovered by Vernalis (compound **54**, a pyrazolylisoxazole). Both companies saw that the binding mode of the second site compound flips in the presence of the compound in the ATP binding site, as seen in Figure 7 by Vernalis for compound **54** in the presence of both **14** and **18**. Astex also saw a second site binder; in their case it was a different bicyclic compound **55**. Of these three companies, only Evotec pursued the fragment linking approach, although there is no report as yet of further progress with compound **31**. Abbott has shown a strong commitment to the fragment linking strategy since their pioneering SAR-by-NMR work of the mid-1990s.[13,14] Again, they discovered an aminopyrimidine compound (**32**) and second-site binders (e.g., **33**) and optimized the compounds by linking (to give **34** and **35**) and by structure-guided growth (**37** and **37**), although there is no report of further progression of these series.

There are a number of points to be made from these examples. The first is that even though the various companies discovered rather similar compounds from a fragment screen, exploiting similar binding motifs, there were no exact matches. The second is that the subsequent evolution of the fragments sometimes took very different paths and produced mostly very different chemical leads and candidates. This emphasizes that more diverse elaboration is possible for a fragment series than is likely from a more elaborated hit derived from conventional HTS screening.

In conclusion, the published Hsp90 programs have demonstrated that not only can a well designed fragment library sample the chemical motifs that can bind to a target but that the chemical diversity available from each fragment is immense. In many ways, finding fragments that bind to a target is a solved problem. The number and quality of hits provide tremendous scope for the imagination of the medicinal chemist working together with the structural biologist and molecular modeler. Perhaps the real challenge is how to identify the most appropriate fragments to progress, and that relies like most drug discovery on experience and skill.

■ ASSOCIATED CONTENT

Supporting Information. Details for the generation of the PDB structures used in this article, list of all structures from this manuscript, Janin 2010 review and the PDB to March 22, 2011 (Table S1), and details of the crystal structures used to prepare Figures 1, 4−9 in this manuscript, including species, chain shown, ligand structure, and crystallographic waters (Table S2). This material is available free of charge via the Internet at http://pubs.acs.org.

■ AUTHOR INFORMATION

Corresponding Author

*Phone: +44-1223-895432. Fax: +44-1223-895556. E-mail: r.hubbard@vernalis.com.

■ BIOGRAPHIES

Stephen D. Roughley obtained his M.A. in 1995 and Ph.D. (with Prof. Andrew B. Holmes, on the modeling and application of nitrone cycloaddition reactions to the synthesis of histrionicotoxin alkaloids) in 1999 from the University of

Cambridge, U.K. During his studies he undertook placements in both Medicinal and Process Chemistry Departments at GlaxoWellcome. In 1999, he joined RiboTargets (later Vernalis) as a medicinal chemist, where he has been involved in a range of drug discovery and technology programs in anti-infective, CNS, and oncology disease areas. Following a secondment in NMR-based fragment screening, he returned to medicinal chemistry as a Principal Scientist and maintains a broad range of interests in drug discovery technologies, medicinal and synthetic chemistry, and cheminformatics.

Roderick E. Hubbard obtained a B.A. (1977) and D.Phil. (1980) in Chemistry from the University of York, U.K. Apart from brief sabbaticals at Harvard University, MA (with Prof. Martin Karplus and Prof. Don Wiley), he has held a series of academic appointments in the Department of Chemistry at University of York, culminating in a Personal Chair in 1995. In the 1980s, he worked on methods for representing and analyzing protein structure. During the 1980s and 1990s he helped develop and directed the York Structural Biology Laboratory. His research interests are in the development and application of structure-based drug discovery methods. Since 2001, he has spent various amounts of his time at the company Vernalis.

■ ACKNOWLEDGMENT

The Hsp90 project was a substantial effort that involved most members of Vernalis at one time or another. Of particular significance for the work presented here were Alan Surgenor in protein crystallization; Lisa Wright in protein crystallography and the recent validation and submission of the Vernalis crystal structures; Xavier Barril, who provided the inspirational contributions in virtual screening and molecular modelling; and Ben Davis who remains the principal driver of the development of the NMR techniques and fragment screening strategies at Vernalis. The early stages of the project were led by Brian Dymock and Harry Finch who were succeeded by Martin Drysdale and Paul Brough in the collaboration with Novartis to the various preclinical candidates. The other members of the Hsp90 team are listed in refs 6, 19, 31, 35, 60, and 80−83. The Hsp90 project was a collaboration with the group of Paul Workman at the ICR for the discovery of NVP-AUY922. Subsequent preclinical and clinical development of NVP-AUY922 and the campaigns that led to NVP-BEP800 were in collaboration with Novartis. The authors are indebted to Yves Janin for the kind provision of the compound structures in his review[24] in electronic format.

■ ABBREVIATIONS USED

ADP, adenosine diphosphate; ADPNP, adenosine 5′-(β,γ-imido)triphosphate; ATP, adenosine triphosphate; Bcl-2, B-cell lymphoma 2; CPMG, Carr−Purcell−Meiboom−Gill NMR T_2 relaxation experiment; D−A, hydrogen bond donor−acceptor; DMPK, drug metabolism and pharmacokinetics; Hsp90, heat shock protein 90; HSQC, heteronuclear single quantum coherence; ICR, Institute for Cancer Research; IP, intellectual property; NMR, nuclear magnetic resonance; Nt-Hsp90, N-terminal domain of Hsp90; PDB, Protein Data Bank (www.rcsb.org); R1, R2, R3, etc., generic groups; SAR, structure−activity relationship; STD, saturation transfer difference

■ REFERENCES

(1) Hopkins, A. L.; Groom, C. R.; Alex, A. Ligand efficiency: a useful metric for lead selection. *Drug Discovery Today* **2004**, *9*, 430–431.

(2) Hajduk, P. J. Fragment-based drug design: how big is too big? *J. Med. Chem.* **2006**, *49*, 6972–6976.

(3) Congreve, M.; Chessari, G.; Tisi, D.; Woodhead, A. J. Recent developments in fragment-based drug discovery. *J. Med. Chem.* **2008**, *51*, 3661–3680.

(4) Chessari, G.; Woodhead, A. J. From fragment to clinical candidate—a historical perspective. *Drug Discovery Today* **2009**, *14*, 668–675.

(5) Schulz, M. N.; Hubbard, R. E. Recent progress in fragment-based lead discovery. *Curr. Opin. Pharmacol.* **2009**, *9*, 615–621.

(6) Baurin, N.; Aboul-Ela, F.; Barril, X.; Davis, B.; Drysdale, M.; Dymock, B.; Finch, H.; Fromont, C.; Richardson, C.; Simmonite, H.; Hubbard, R. E. Design and characterization of libraries of molecular fragments for use in NMR screening against protein targets. *J. Chem. Inf. Comput. Sci.* **2004**, *44*, 2157–2166.

(7) Chen, I. J.; Hubbard, R. E. Lessons for fragment library design: analysis of output from multiple screening campaigns. *J. Comput.-Aided Mol. Des.* **2009**, *23*, 603–620.

(8) Albert, J. S.; Blomberg, N.; Breeze, A. L.; Brown, A. J.; Burrows, J. N.; Edwards, P. D.; Folmer, R. H.; Geschwindner, S.; Griffen, E. J.; Kenny, P. W.; Nowak, T.; Olsson, L. L.; Sanganee, H.; Shapiro, A. B. An integrated approach to fragment-based lead generation: philosophy, strategy and case studies from AstraZeneca's drug discovery programmes. *Curr. Top. Med. Chem.* **2007**, *7*, 1600–1629.

(9) Fischer, M.; Hubbard, R. E. Fragment-based ligand discovery. *Mol. Interventions* **2009**, *9*, 22–30.

(10) Murray, C. W.; Blundell, T. L. Structural biology in fragment-based drug design. *Curr. Opin. Struct. Biol.* **2010**, *20*, 497–507.

(11) Hubbard, R.; Murray, J. B. Experiences in fragment-based lead discovery. *Methods Enzymol.* **2011**, *493*, 509–531.

(12) Erlanson, D. A. Fragment-based lead discovery: a chemical update. *Curr. Opin. Biotechnol.* **2006**, *17*, 643–652.

(13) Shuker, S. B.; Hajduk, P. J.; Meadows, R. P.; Fesik, S. W. Discovering high-affinity ligands for proteins: SAR by NMR. *Science* **1996**, *274*, 1531–1534.

(14) Hajduk, P. J. SAR by NMR: putting the pieces together. *Mol. Interventions* **2006**, *6*, 266–272.

(15) Huth, J. R.; Park, C.; Petros, A. M.; Kunzer, A. R.; Wendt, M. D.; Wang, X.; Lynch, C. L.; Mack, J. C.; Swift, K. M.; Judge, R. A.; Chen, J.; Richardson, P. L.; Jin, S.; Tahir, S. K.; Matayoshi, E. D.; Dorwin, S. A.; Ladror, U. S.; Severin, J. M.; Walter, K. A.; Bartley, D. M.; Fesik, S. W.; Elmore, S. W.; Hajduk, P. J. Discovery and design of novel HSP90 inhibitors using multiple fragment-based design strategies. *Chem. Biol. Drug Des.* **2007**, *70*, 1–12.

(16) Petros, A. M.; Huth, J. R.; Oost, T.; Park, C. M.; Ding, H.; Wang, X.; Zhang, H.; Nimmer, P.; Mendoza, R.; Sun, C.; Mack, J.; Walter, K.; Dorwin, S.; Gramling, E.; Ladror, U.; Rosenberg, S. H.; Elmore, S. W.; Fesik, S. W.; Hajduk, P. J. Discovery of a potent and selective Bcl-2 inhibitor using SAR by NMR. *Bioorg. Med. Chem. Lett.* **2010**, *20*, 6587–6591.

(17) Howard, S.; Berdini, V.; Boulstridge, J. A.; Carr, M. G.; Cross, D. M.; Curry, J.; Devine, L. A.; Early, T. R.; Fazal, L.; Gill, A. L.; Heathcote, M.; Maman, S.; Matthews, J. E.; McMenamin, R. L.; Navarro, E. F.; O'Brien, M. A.; O'Reilly, M.; Rees, D. C.; Reule, M.; Tisi, D.; Williams, G.; Vinkovic, M.; Wyatt, P. G. Fragment-based discovery of the pyrazol-4-yl urea (AT9283), a multitargeted kinase inhibitor with potent aurora kinase activity. *J. Med. Chem.* **2009**, *52*, 379–388.

(18) McHardy, T.; Caldwell, J. J.; Cheung, K. M.; Hunter, L. J.; Taylor, K.; Rowlands, M.; Ruddle, R.; Henley, A.; de Haven Brandon, A.; Valenti, M.; Davies, T. G.; Fazal, L.; Seavers, L.; Raynaud, F. I.; Eccles, S. A.; Aherne, G. W.; Garrett, M. D.; Collins, I. Discovery of 4-amino-1-(7*H*-pyrrolo[2,3-*d*]-pyrimidin-4-yl)piperidine-4-carboxamides as selective, orally active inhibitors of protein kinase B (Akt). *J. Med. Chem.* **2010**, *53*, 2239–2249.

(19) Brough, P. A.; Barril, X.; Borgognoni, J.; Chene, P.; Davies, N. G.; Davis, B.; Drysdale, M. J.; Dymock, B.; Eccles, S. A.; Garcia-Echeverria, C.; Fromont, C.; Hayes, A.; Hubbard, R. E.; Jordan, A. M.;

Jensen, M. R.; Massey, A.; Merrett, A.; Padfield, A.; Parsons, R.; Radimerski, T.; Raynaud, F. I.; Robertson, A.; Roughley, S. D.; Schoepfer, J.; Simmonite, H.; Sharp, S. Y.; Surgenor, A.; Valenti, M.; Walls, S.; Webb, P.; Wood, M.; Workman, P.; Wright, L. Combining hit identification strategies: fragment-based and in silico approaches to orally active 2-aminothieno[2,3-*d*]pyrimidine inhibitors of the Hsp90 molecular chaperone. *J. Med. Chem.* **2009**, *52*, 4794–4809.

(20) Hubbard, R. E. Fragment approaches in structure-based drug discovery. *J. Synchrotron Radiat.* **2008**, *15*, 227–230.

(21) Mochalkin, I.; Miller, J. R.; Narasimhan, L.; Thanabal, V.; Erdman, P.; Cox, P. B.; Prasad, J. V.; Lightle, S.; Huband, M. D.; Stover, C. K. Discovery of antibacterial biotin carboxylase inhibitors by virtual screening and fragment-based approaches. *ACS Chem. Biol.* **2009**, *4*, 473–483.

(22) Fink, T.; Reymond, J. L. Virtual exploration of the chemical universe up to 11 atoms of C, N, O, F: assembly of 26.4 million structures (110.9 million stereoisomers) and analysis for new ring systems, stereochemistry, physicochemical properties, compound classes, and drug discovery. *J. Chem. Inf. Model.* **2007**, *47*, 342–353.

(23) Biamonte, M. A.; Van de Water, R.; Arndt, J. W.; Scannevin, R. H.; Perret, D.; Lee, W. C. Heat shock protein 90: inhibitors in clinical trials. *J. Med. Chem.* **2010**, *53*, 3–17.

(24) Janin, Y. L. ATPase inhibitors of heat-shock protein 90, second season. *Drug Discovery Today* **2010**, *15*, 342–353.

(25) Pearl, L. H.; Prodromou, C. Structure and mechanism of the Hsp90 molecular chaperone machinery. *Annu. Rev. Biochem.* **2006**, *75*, 271–294.

(26) Dutta, R.; Inouye, M. GHKL, an emergent ATPase/kinase superfamily. *Trends Biochem. Sci.* **2000**, *25*, 24–28.

(27) Chiosis, G.; Timaul, M. N.; Lucas, B.; Munster, P. N.; Zheng, F. F.; Sepp-Lorenzino, L.; Rosen, N. A small molecule designed to bind to the adenine nucleotide pocket of Hsp90 causes Her2 degradation and the growth arrest and differentiation of breast cancer cells. *Chem. Biol.* **2001**, *8*, 289–299.

(28) Gao, Z.; Garcia-Echeverria, C.; Jensen, M. R. Hsp90 inhibitors: clinical development and future opportunities in oncology therapy. *Curr. Opin. Drug Discovery Dev.* **2010**, *13*, 193–202.

(29) Hanahan, D.; Weinberg, R. A. The hallmarks of cancer. *Cell* **2000**, *100*, 57–70.

(30) Stebbins, C. E.; Russo, A. A.; Schneider, C.; Rosen, N.; Hartl, F. U.; Pavletich, N. P. Crystal structure of an Hsp90-geldanamycin complex: targeting of a protein chaperone by an antitumor agent. *Cell* **1997**, *89*, 239–250.

(31) Dymock, B.; Barril, X.; Beswick, M.; Collier, A.; Davies, N.; Drysdale, M.; Fink, A.; Fromont, C.; Hubbard, R. E.; Massey, A.; Surgenor, A.; Wright, L. Adenine derived inhibitors of the molecular chaperone HSP90-SAR explained through multiple X-ray structures. *Bioorg. Med. Chem. Lett.* **2004**, *14*, 325–328.

(32) Barta, T. E.; Veal, J. M.; Rice, J. W.; Partridge, J. M.; Fadden, R. P.; Ma, W.; Jenks, M.; Geng, L.; Hanson, G. J.; Huang, K. H.; Barabasz, A. F.; Foley, B. E.; Otto, J.; Hall, S. E. Discovery of benzamide tetrahydro-4*H*-carbazol-4-ones as novel small molecule inhibitors of Hsp90. *Bioorg. Med. Chem. Lett.* **2008**, *18*, 3517–3521.

(33) Taldone, T.; Gozman, A.; Maharaj, R.; Chiosis, G. Targeting Hsp90: small-molecule inhibitors and their clinical development. *Curr. Opin. Pharmacol.* **2008**, *8*, 370–374.

(34) Eccles, S. A.; Massey, A.; Raynaud, F. I.; Sharp, S. Y.; Box, G.; Valenti, M.; Patterson, L.; de Haven Brandon, A.; Gowan, S.; Boxall, F.; Aherne, W.; Rowlands, M.; Hayes, A.; Martins, V.; Urban, F.; Boxall, K.; Prodromou, C.; Pearl, L.; James, K.; Matthews, T. P.; Cheung, K. M.; Kalusa, A.; Jones, K.; McDonald, E.; Barril, X.; Brough, P. A.; Cansfield, J. E.; Dymock, B.; Drysdale, M. J.; Finch, H.; Howes, R.; Hubbard, R. E.; Surgenor, A.; Webb, P.; Wood, M.; Wright, L.; Workman, P. NVP-AUY922: a novel heat shock protein 90 inhibitor active against xenograft tumor growth, angiogenesis, and metastasis. *Cancer Res.* **2008**, *68*, 2850–2860.

(35) Brough, P. A.; Aherne, W.; Barril, X.; Borgognoni, J.; Boxall, K.; Cansfield, J. E.; Cheung, K. M.; Collins, I.; Davies, N. G.; Drysdale, M. J.; Dymock, B.; Eccles, S. A.; Finch, H.; Fink, A.; Hayes, A.; Howes, R.; Hubbard, R. E.; James, K.; Jordan, A. M.; Lockie, A.; Martins, V.; Massey, A.; Matthews, T. P.; McDonald, E.; Northfield, C. J.; Pearl, L. H.; Prodromou, C.; Ray, S.; Raynaud, F. I.; Roughley, S. D.; Sharp, S. Y.; Surgenor, A.; Walmsley, D. L.; Webb, P.; Wood, M.; Workman, P.; Wright, L. 4,5-Diarylisoxazole Hsp90 chaperone inhibitors: potential therapeutic agents for the treatment of cancer. *J. Med. Chem.* **2008**, *51*, 196–218.

(36) Lundgren, K.; Zhang, H.; Brekken, J.; Huser, N.; Powell, R. E.; Timple, N.; Busch, D. J.; Neely, L.; Sensintaffar, J. L.; Yang, Y. C.; McKenzie, A.; Friedman, J.; Scannevin, R.; Kamal, A.; Hong, K.; Kasibhatla, S. R.; Boehm, M. F.; Burrows, F. J. BIIB021, an orally available, fully synthetic small-molecule inhibitor of the heat shock protein Hsp90. *Mol. Cancer Ther.* **2009**, *8*, 921–929.

(37) Wang, Y.; Trepel, J. B.; Neckers, L. M.; Giaccone, G. STA-9090, a small-molecule Hsp90 inhibitor for the potential treatment of cancer. *Curr. Opin. Invest. Drugs* **2010**, *11*, 1466–1476.

(38) Huang, K. H.; Veal, J. M.; Fadden, R. P.; Rice, J. W.; Eaves, J.; Strachan, J. P.; Barabasz, A. F.; Foley, B. E.; Barta, T. E.; Ma, W.; Silinski, M. A.; Hu, M.; Partridge, J. M.; Scott, A.; DuBois, L. G.; Freed, T.; Steed, P. M.; Ommen, A. J.; Smith, E. D.; Hughes, P. F.; Woodward, A. R.; Hanson, G. J.; McCall, W. S.; Markworth, C. J.; Hinkley, L.; Jenks, M.; Geng, L.; Lewis, M.; Otto, J.; Pronk, B.; Verleysen, K.; Hall, S. E. Discovery of novel 2-aminobenzamide inhibitors of heat shock protein 90 as potent, selective and orally active antitumor agents. *J. Med. Chem.* **2009**, *52*, 4288–4305.

(39) Woodhead, A. J.; Angove, H.; Carr, M. G.; Chessari, G.; Congreve, M.; Coyle, J. E.; Cosme, J.; Graham, B.; Day, P. J.; Downham, R.; Fazal, L.; Feltell, R.; Figueroa, E.; Frederickson, M.; Lewis, J.; McMenamin, R.; Murray, C. W.; O'Brien, M. A.; Parra, L.; Patel, S.; Phillips, T.; Rees, D. C.; Rich, S.; Smith, D. M.; Trewartha, G.; Vinkovic, M.; Williams, B.; Woolford, A. J. Discovery of (2,4-dihydroxy-5-isopropylphenyl)-[5-(4-methylpiperazin-1-ylmethyl)-1,3-dihydroisoindol-2-yl]methanone (AT13387), a novel inhibitor of the molecular chaperone Hsp90 by fragment based drug design. *J. Med. Chem.* **2010**, *53*, 5956–5969.

(40) Mayer, M.; Meyer, B. Characterization of ligand binding by saturation transfer difference NMR spectroscopy. *Angew. Chem., Int. Ed.* **1999**, *38*, 1784–1788.

(41) Chiosis, G.; Lucas, B.; Huezo, H.; Solit, D.; Basso, A.; Rosen, N. Development of purine-scaffold small molecule inhibitors of Hsp90. *Curr. Cancer Drug Targets* **2003**, *3*, 371–376.

(42) Hubbard, R. E.; Davis, B.; Chen, I.; Drysdale, M. J. The SeeDs approach: integrating fragments into drug discovery. *Curr. Top. Med. Chem.* **2007**, *7*, 1568–1581.

(43) Dalvit, C.; Pevarello, P.; Tatò, M.; Veronesi, M.; Vulpetti, A.; Sundström, M. Identification of compounds with binding affinity to proteins via magnetization transfer from bulk water. *J. Biomol. NMR* **2000**, *18*, 65–68.

(44) Meiboom, S.; Gill, D. Modified spin-echo method for measuring nuclear relaxation times. *Rev. Sci. Instrum.* **1958**, *29*, 688–691.

(45) Bao, R.; Lai, C. J.; Qu, H.; Wang, D.; Yin, L.; Zifcak, B.; Atoyan, R.; Wang, J.; Samson, M.; Forrester, J.; DellaRocca, S.; Xu, G. X.; Tao, X.; Zhai, H. X.; Cai, X.; Qian, C. CUDC-305, a novel synthetic HSP90 inhibitor with unique pharmacologic properties for cancer therapy. *Clin. Cancer Res.* **2009**, *15*, 4046–4057.

(46) Bao, R.; Lai, C. J.; Wang, D. G.; Qu, H.; Yin, L.; Zifcak, B.; Tao, X.; Wang, J.; Atoyan, R.; Samson, M.; Forrester, J.; Xu, G. X.; DellaRocca, S.; Borek, M.; Zhai, H. X.; Cai, X.; Qian, C. Targeting heat shock protein 90 with CUDC-305 overcomes erlotinib resistance in non-small cell lung cancer. *Mol. Cancer Ther.* **2009**, *8*, 3296–3306.

(47) Kung, P. P.; Huang, B.; Zhang, G.; Zhou, J. Z.; Wang, J.; Digits, J. A.; Skaptason, J.; Yamazaki, S.; Neul, D.; Zientek, M.; Elleraas, J.; Mehta, P.; Yin, M. J.; Hickey, M. J.; Gajiwala, K. S.; Rodgers, C.; Davies, J. F.; Gehring, M. R. Dihydroxyphenylisoindoline amides as orally bioavailable inhibitors of the heat shock protein 90 (hsp90) molecular chaperone. *J. Med. Chem.* **2010**, *53*, 499–503.

(48) Usmani, S. Z.; Bona, R.; Li, Z. 17 AAG for HSP90 inhibition in cancer—from bench to bedside. *Curr. Mol. Med.* **2009**, *9*, 654–664.

(49) Hanson, B. E.; Vesole, D. H. Retaspimycin hydrochloride (IPI-504): a novel heat shock protein inhibitor as an anticancer agent. *Expert Opin. Invest. Drugs* **2009**, *18*, 1375–1383.

(50) Taldone, T.; Sun, W.; Chiosis, G. Discovery and development of heat shock protein 90 inhibitors. *Bioorg. Med. Chem.* **2009**, *17*, 2225–2235.

(51) Kasibhatla, S. R.; Hong, K.; Biamonte, M. A.; Busch, D. J.; Karjian, P. L.; Sensintaffar, J. L.; Kamal, A.; Lough, R. E.; Brekken, J.; Lundgren, K.; Grecko, R.; Timony, G. A.; Ran, Y.; Mansfield, R.; Fritz, L. C.; Ulm, E.; Burrows, F. J.; Boehm, M. F. Rationally designed high-affinity 2-amino-6-halopurine heat shock protein 90 inhibitors that exhibit potent antitumor activity. *J. Med. Chem.* **2007**, *50*, 2767–2778.

(52) Zagorska, A.; Jurczyk, S.; Pawlowski, M.; Dybala, M.; Nowak, G.; Tatarczynska, E.; Nikiforuk, A.; Chojnacka-Wojcik, E. Synthesis and preliminary pharmacological evaluation of imidazo[2,1-*f*]purine-2,4-dione derivatives. *Eur. J. Med. Chem.* **2009**, *44*, 4288–4296.

(53) Murray, C. W.; Carr, M. G.; Callaghan, O.; Chessari, G.; Congreve, M.; Cowan, S.; Coyle, J. E.; Downham, R.; Figueroa, E.; Frederickson, M.; Graham, B.; McMenamin, R.; O'Brien, M. A.; Patel, S.; Phillips, T. R.; Williams, G.; Woodhead, A. J.; Woolford, A. J. Fragment-based drug discovery applied to Hsp90. Discovery of two lead series with high ligand efficiency. *J. Med. Chem.* **2010**, *53*, 5942–5955.

(54) Barker, J. J.; Barker, O.; Boggio, R.; Chauhan, V.; Cheng, R. K.; Corden, V.; Courtney, S. M.; Edwards, N.; Falque, V. M.; Fusar, F.; Gardiner, M.; Hamelin, E. M.; Hesterkamp, T.; Ichihara, O.; Jones, R. S.; Mather, O.; Mercurio, C.; Minucci, S.; Montalbetti, C. A.; Muller, A.; Patel, D.; Phillips, B. G.; Varasi, M.; Whittaker, M.; Winkler, D.; Yarnold, C. J. Fragment-based identification of Hsp90 inhibitors. *ChemMedChem* **2009**, *4*, 963–966.

(55) Barker, J. J.; Barker, O.; Courtney, S. M.; Gardiner, M.; Hesterkamp, T.; Ichihara, O.; Mather, O.; Montalbetti, C. A.; Muller, A.; Varasi, M.; Whittaker, M.; Yarnold, C. J. Discovery of a novel Hsp90 inhibitor by fragment linking. *ChemMedChem* **2010**, *5*, 1697–1700.

(56) Boehm, H. J.; Boehringer, M.; Bur, D.; Gmuender, H.; Huber, W.; Klaus, W.; Kostrewa, D.; Kuehne, H.; Luebbers, T.; Meunier-Keller, N.; Mueller, F. Novel inhibitors of DNA gyrase: 3D structure based biased needle screening, hit validation by biophysical methods, and 3D guided optimization. A promising alternative to random screening. *J. Med. Chem.* **2000**, *43*, 2664–2674.

(57) Kung, P. P.; Funk, L.; Meng, J.; Collins, M.; Zhou, J. Z.; Johnson, M. C.; Ekker, A.; Wang, J.; Mehta, P.; Yin, M. J.; Rodgers, C.; Davies, J. F., 2nd; Bayman, E.; Smeal, T.; Maegley, K. A.; Gehring, M. R. Dihydroxylphenyl amides as inhibitors of the Hsp90 molecular chaperone. *Bioorg. Med. Chem. Lett.* **2008**, *18*, 6273–6278.

(58) Cho-Schultz, S.; Patten, M. J.; Huang, B.; Elleraas, J.; Gajiwala, K. S.; Hickey, M. J.; Wang, J.; Mehta, P. P.; Kang, P.; Gehring, M. R.; Kung, P.-P.; Sutton, S. C. Solution-phase parallel synthesis of Hsp90 inhibitors. *J. Comb. Chem.* **2009**, *11*, 860–874.

(59) Cheung, K. M.; Matthews, T. P.; James, K.; Rowlands, M. G.; Boxall, K. J.; Sharp, S. Y.; Maloney, A.; Roe, S. M.; Prodromou, C.; Pearl, L. H.; Aherne, G. W.; McDonald, E.; Workman, P. The identification, synthesis, protein crystal structure and in vitro biochemical evaluation of a new 3,4-diarylpyrazole class of Hsp90 inhibitors. *Bioorg. Med. Chem. Lett.* **2005**, *15*, 3338–3343.

(60) Barril, X.; Brough, P.; Drysdale, M.; Hubbard, R. E.; Massey, A.; Surgenor, A.; Wright, L. Structure-based discovery of a new class of Hsp90 inhibitors. *Bioorg. Med. Chem. Lett.* **2005**, *15*, 5187–5191.

(61) Barluenga, S.; Fontaine, J.-G.; Wang, C.; Aouadi, K.; Chen, R.; Beebe, K.; Neckers, L.; Winssinger, N. Inhibition of HSP90 with pochoximes: SAR and structure-based insights. *ChemBioChem* **2009**, *10*, 2753–2759.

(62) Zhang, M.-Q.; Gaisser, S.; Nur-E-Alam, M.; Sheehan, L. S.; Vousden, W. A.; Gaitatzis, N.; Peck, G.; Coates, N. J.; Moss, S. J.; Radzom, M.; Foster, T. A.; Sheridan, R. M.; Gregory, M. A.; Roe, S. M.; Prodromou, C.; Pearl, L.; Boyd, S. M.; Wilkinson, B.; Martin, C. J. Optimizing natural products by biosynthetic engineering: discovery of nonquinone Hsp90 inhibitors. *J. Med. Chem.* **2008**, *51*, 5494–5497.

(63) Immormino, R. M.; Kang, Y.; Chiosis, G.; Gewirth, D. T. Structural and quantum chemical studies of 8-aryl-sulfanyl adenine class Hsp90 inhibitors. *J. Med. Chem.* **2006**, *49*, 4953–4960.

(64) Southall, N. T.; Ajay Kinase patent space visualization using chemical replacements. *J. Med. Chem.* **2006**, *49*, 2103–2109.

(65) Fleming, F. F.; Yao, L.; Ravikumar, P. C.; Funk, L.; Shook, B. C. Nitrile-containing pharmaceuticals: efficacious roles of the nitrile pharmacophore. *J. Med. Chem.* **2010**, *53*, 7902–7917.

(66) Olejniczak, E. T.; Hajduk, P. J.; Marcotte, P. A.; Nettesheim, D. G.; Meadows, R. P.; Edalji, R.; Holzman, T. F.; Fesik, S. W. Stromelysin inhibitors designed from weakly bound fragments: effects of linking and cooperativity. *J. Am. Chem. Soc.* **1997**, *119*, 5828–5832.

(67) Bamborough, P.; Angell, R. M.; Bhamra, I.; Brown, D.; Bull, J.; Christopher, J. A.; Cooper, A. W. J.; Fazal, L. H.; Giordano, I.; Hind, L.; Patel, V. K.; Ranshaw, L. E.; Sims, M. J.; Skone, P. A.; Smith, K. J.; Vickerstaff, E.; Washington, M. *N*-4-Pyrimidinyl-1*H*-indazol-4-amine inhibitors of Lck: indazoles as phenol isosteres with improved pharmacokinetics. *Bioorg. Med. Chem. Lett.* **2007**, *17*, 4363–4368.

(68) Folkes, A. J.; Ahmadi, K.; Alderton, W. K.; Alix, S.; Baker, S. J.; Box, G.; Chuckowree, I. S.; Clarke, P. A.; Depledge, P.; Eccles, S. A.; Friedman, L. S.; Hayes, A.; Hancox, T. C.; Kugendradas, A.; Lensun, L.; Moore, P.; Olivero, A. G.; Pang, J.; Patel, S.; Pergl-Wilson, G. H.; Raynaud, F. I.; Robson, A.; Saghir, N.; Salphati, L.; Sohal, S.; Ultsch, M. H.; Valenti, M.; Wallweber, H. J. A.; Wan, N. C.; Wiesmann, C.; Workman, P.; Zhyvoloup, A.; Zvelebil, M. J.; Shuttleworth, S. J. The identification of 2-(1*H*-indazol-4-yl)-6-(4-methanesulfonyl-piperazin-1-ylmethyl)-4-morpholin-4-yl-thieno[3,2-*d*]pyrimidine (GDC-0941) as a potent, selective, orally bioavailable inhibitor of class I PI3 kinase for the treatment of cancer. *J. Med. Chem.* **2008**, *51*, 5522–5532.

(69) Collin, D. T.; Hartley, D.; Jack, D.; Lunts, L. H.; Press, J. C.; Ritchie, A. C.; Toon, P. Saligenin analogs of sympathomimetic catecholamines. *J. Med. Chem.* **1970**, *13*, 674–680.

(70) Brittain, R. T.; Farmer, J. B.; Jack, D.; Martin, L. E.; Simpson, W. T. Alpha-[(*t*-Butylamino)methyl]-4-hydroxy-*m*-xylene-alpha 1,alpha 3-diol (AH.3365): a selective beta-adrenergic stimulant. *Nature* **1968**, *219*, 862–863.

(71) Kuhn, B.; Mohr, P.; Stahl, M. Intramolecular hydrogen bonding in medicinal chemistry. *J. Med. Chem.* **2010**, *53*, 2601–2611.

(72) Bi, W.; Bi, L.; Cai, J.; Liu, S.; Peng, S.; Fischer, N. O.; Tok, J. B. H.; Wang, G. Dual-acting agents that possess free radical scavenging and antithrombotic activities: design, synthesis, and evaluation of phenolic tetrahydro-[beta]-carboline RGD peptide conjugates. *Bioorg. Med. Chem. Lett.* **2006**, *16*, 4523–4527.

(73) Legeay, J. C.; Vanden Eynde, J. J.; Bazureau, J. P. A new approach to N-3 functionalized 3,4-dihydropyrimidine-2(1*H*)-ones with 1,2,4-oxadiazole group as amide isostere via ionic liquid-phase technology. *Tetrahedron Lett.* **2007**, *48*, 1063–1068.

(74) de Kloe, G. E.; Retra, K.; Geitmann, M.; Kallblad, P.; Nahar, T.; van Elk, R.; Smit, A. B.; van Muijlwijk-Koezen, J. E.; Leurs, R.; Irth, H.; Danielson, U. H.; de Esch, I. J. P. Surface plasmon resonance biosensor based fragment screening using acetylcholine binding protein identifies ligand efficiency hot spots (LE hot spots) by deconstruction of nicotinic acetylcholine receptor α7 ligands. *J. Med. Chem.* **2010**, *53*, 7192–7201.

(75) Barelier, S.; Pons, J.; Marcillat, O.; Lancelin, J.-M.; Krimm, I. Fragment-based deconstruction of Bcl-xL inhibitors. *J. Med. Chem.* **2010**, *53*, 2577–2588.

(76) Petros, A. M.; Dinges, J.; Augeri, D. J.; Baumeister, S. A.; Betebenner, D. A.; Bures, M. G.; Elmore, S. W.; Hajduk, P. J.; Joseph, M. K.; Landis, S. K.; Nettesheim, D. G.; Rosenberg, S. H.; Shen, W.; Thomas, S.; Wang, X.; Zanze, I.; Zhang, H.; Fesik, S. W. Discovery of a potent inhibitor of the antiapoptotic protein Bcl-xL from NMR and parallel synthesis. *J. Med. Chem.* **2005**, *49*, 656–663.

(77) Tounge, B. A.; Parker, M. H. Designing a diverse high-quality library for crystallography-based FBDD screening. *Methods Enzymol.* **2011**, *493*, 3–20.

(78) Kung, P.-P.; Huang, B.; Zhang, G.; Zhou, J. Z.; Wang, J.; Digits, J. A.; Skaptason, J.; Yamazaki, S.; Neul, D.; Zientek, M.; Elleraas, J.; Mehta, P.; Yin, M.-J.; Hickey, M. J.; Gajiwala, K. S.; Rodgers, C.; Davies,

J. F.; Gehring, M. R. Dihydroxyphenylisoindoline amides as orally bioavailable inhibitors of the heat shock protein 90 (Hsp90) molecular chaperone. *J. Med. Chem.* **2009**, *53*, 499–503.

(79) Mehta, P. P.; Kung, P.-P.; Yamazaki, S.; Walls, M.; Shen, A.; Nguyen, L.; Gehring, M. R.; Los, G.; Smeal, T.; Yin, M.-J. A novel class of specific Hsp90 small molecule inhibitors demonstrate in vitro and in vivo anti-tumor activity in human melanoma cells. *Cancer Lett.* **2011**, *300*, 30–39.

(80) Wright, L.; Barril, X.; Dymock, B.; Sheridan, L.; Surgenor, A.; Beswick, M.; Drysdale, M.; Collier, A.; Massey, A.; Davies, N.; Fink, A.; Fromont, C.; Aherne, W.; Boxall, K.; Sharp, S.; Workman, P.; Hubbard, R. E. Structure−activity relationships in purine-based inhibitor binding to HSP90 isoforms. *Chem. Biol.* **2004**, *11*, 775–785.

(81) Brough, P. A.; Barril, X.; Beswick, M.; Dymock, B. W.; Drysdale, M. J.; Wright, L.; Grant, K.; Massey, A.; Surgenor, A.; Workman, P. 3-(5-Chloro-2,4-dihydroxyphenyl)-pyrazole-4-carboxamides as inhibitors of the Hsp90 molecular chaperone. *Bioorg. Med. Chem. Lett.* **2005**, *15*, 5197–5201.

(82) Dymock, B. W.; Barril, X.; Brough, P. A.; Cansfield, J. E.; Massey, A.; McDonald, E.; Hubbard, R. E.; Surgenor, A.; Roughley, S. D.; Webb, P.; Workman, P.; Wright, L.; Drysdale, M. J. Novel, potent small-molecule inhibitors of the molecular chaperone Hsp90 discovered through structure-based design. *J. Med. Chem.* **2005**, *48*, 4212–4215.

(83) Howes, R.; Barril, X.; Dymock, B. W.; Grant, K.; Northfield, C. J.; Robertson, A. G.; Surgenor, A.; Wayne, J.; Wright, L.; James, K.; Matthews, T.; Cheung, K. M.; McDonald, E.; Workman, P.; Drysdale, M. J. A fluorescence polarization assay for inhibitors of Hsp90. *Anal. Biochem.* **2006**, *350*, 202–213.